

Potential Capacity and Cost of Pumped-Storage Power in Japan (Vol. 3)

Summary

The 2019 paper puts forward *new pumped storage power* as a system for storing power from renewables, a major source of electricity in a zero-carbon society[1]. This new system calls for utilizing an existing multipurpose dam for a lower reservoir and constructing plural smaller upper reservoirs and power plants. The 2020 paper estimates the total potential storage capacity under this system in Japan at 750-2,200 GWh/cycle/day without considering individual topographic conditions[2]. In this paper we consider more realistic conditions, including local topography and land use regulations, in reassessing the potential capacity and power generation cost of a feasible new pumped storage power plant. We conclude new pumped storage power offering a viable power storage solution for the future.

Proposals for Policy Development

- Potential storage capacity that can be developed is expected to be 585-1,392 GWh/cycle/day, well above 510 GWh/cycle/day[3], a level that needs to be secured by 2050. The power generation cost is estimated at 18.5-20.5 JPY/kWh.
- Potential sites are widely distributed across the country. It is necessary to investigate site suitability of pumped storage power plants in each region and an optimal renewable energy combination with the plants. Development plan should be proceeded according to the investigation.
- A smaller dam means easier with which to pinpoint the sites for upper reservoirs, as well as easier and less costly construction. As a development procedure, it is preferable to begin with smaller dams.
- Water stored in a multipurpose dam is used for various purposes. It is thus important to ensure that water use for pumped storage power does not undermine the functions of water utilization and flood control of the dam.

1. Distribution of New Pumped Storage Power Plants

A new pumped storage power plant involves plural upper reservoirs and power plants of the same specifications (Figure 1). The power storage capacity of such a plant depends on the scale of the multipurpose dam (lower reservoir). A total of 931 multipurpose dams in Japan that can serve as lower reservoirs are classified into five categories according to their scale (water storage capacity) to assess the distribution of potential sites. The findings are shown in Figure 2.

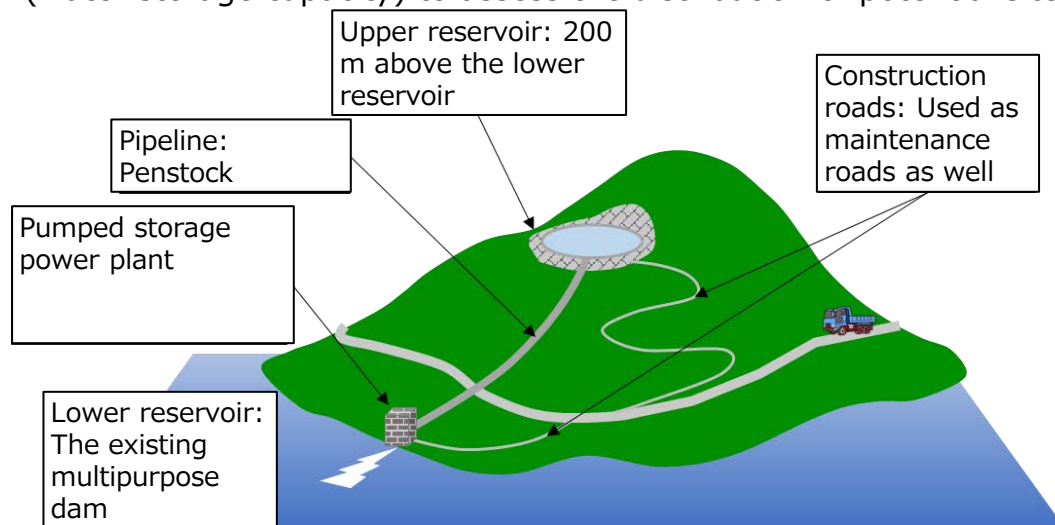


Figure 1 Schematic Diagram of a New Pumped Storage Power

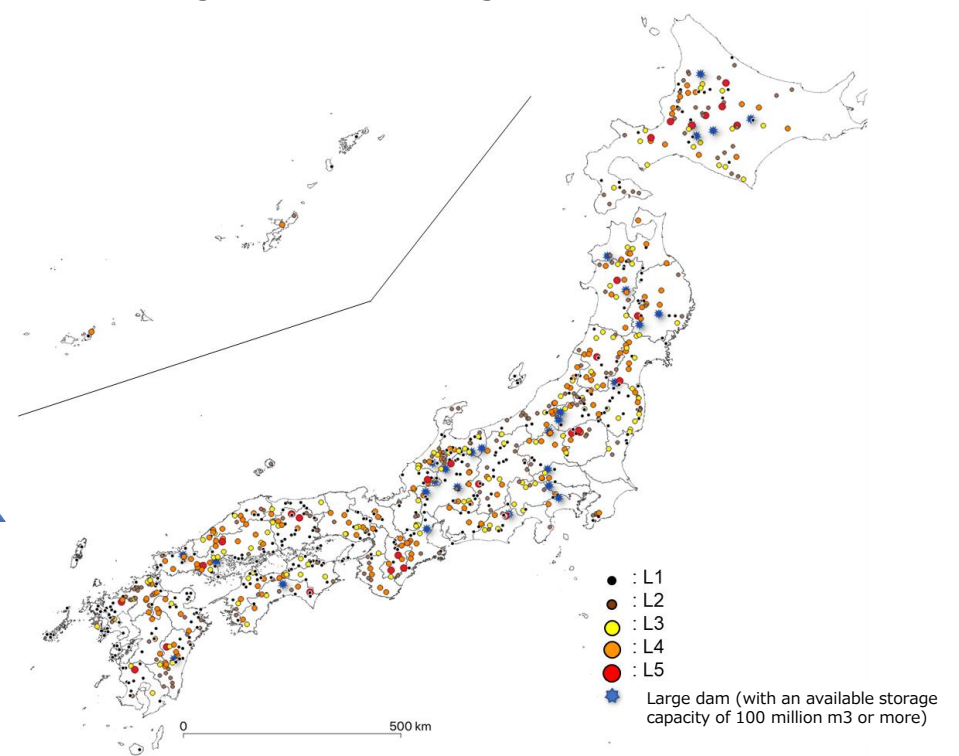


Figure 2 Locations of New Pumped Storage Power Plants in Japan

2. The Construction Cost of a New Pumped Storage Power Plant

Detailed estimation that factored in topography and other conditions has found that the total construction cost of a new pumped storage power plant will be 2.73 billion JPY. For 80% of such stations, the cost will range from 2.5 to 3 billion JPY. The steeper the upper reservoir site and the longer the pipeline, the higher the construction cost.

The cost of leveling land and constructing upper reservoirs accounts for more than 50% of the total construction cost (Figure 3).

3. Estimates under Different Conditions

Table 1 shows the estimates of power generation cost and potential storage capacity under different conditions in comparison with those used in the 2020 paper[2] (Plan 0). Plan 1 considers more accurate topographic conditions. Plans 2-5 also reflect two other factors: the ratio of water usage to the available water storage capacity of the dam and whether or not a large dam is involved.

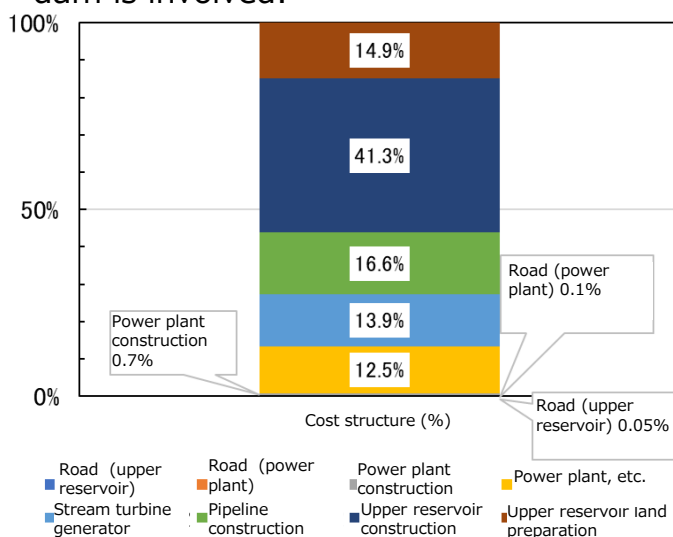


Figure 3 Structure of the Cost of a New Pumped Storage Power Plant

Table 1 Potential Storage Capacity and Cost of a New Pumped Storage Power Plant

Plan	Topographic conditions considered or not	A. Ratio of water usage to effective storage capacity (%)	B. Large dam (with an available water storage capacity of 100 million m3 or more) involved?	C. Facility cost (JPY/Wh)	D. Power generation cost (JPY/kWh)	E. Installed storage capacity (MWh/power-house/cycle/day)	F. Total no. of dams	G. Total no. of upper reservoirs that can be constructed	H. National total of installed storage capacity (GWh/cycle/day)	I. Average installed storage capacity (GWh/cycle/day)	J. National total of annual installed storage capacity (TWh/year)
0	No(*)	20	No	44.5	20.4	61	1000	14900	907	0.91	272
1	Yes	20	No	44.9	20.5	61	931	9640	585	0.63	176
2	Yes	30	No	34.9	18.5	91	931	9640	878	0.94	263
3	Yes	20	Yes	44.9	20.5	61	959	15280	928	0.97	278
4	Yes	30	Yes	34.9	18.5	91	959	15280	1392	1.45	417
5	Yes	20(**)	No	40.9	19.7	70	931	9640	655	0.7	196

(*)No (Assumptions: 20% of stored water can all be used for pumped storage power and all pumped storage power plants share the same specifications, i.e., Plan A in the 2019 proposal paper[2])
 (**) 20 (or 30 for Hokkaido and Tohoku)

[1] LCS, "Potential Capacity and Cost of Pumped-Storage Power in Japan," Proposal Paper for Policy Making and Governmental Action toward Low Carbon Societies, January, 2019.
 [2] LCS, "Potential Capacity and Cost of Pumped-Storage Power in Japan (Vol. 2)," Proposal Paper for Policy Making and Governmental Action toward Low Carbon Societies, February, 2020.
 [3] LCS, "Economic Evaluation for Low Carbon Electric Power System Considering System Stability (Vol. 2)," Proposal Paper for Policy Making and Governmental Action toward Low Carbon Societies, March 2018.



SOFC Systems (Vol. 8): Evaluations of Energy Conversion and Utilization Technologies for Hydrogen Economy

Summary

Renewable hydrogen stations have been attracting attention recently. These stations supply CO₂-free hydrogen by conducting water electrolysis in a hydrogen production unit using renewable-derived electric power. In this proposal paper, a hydrogen station that adopts a hydrogen production system using fuel cells and renewables (SOEC system) was designed, and the costs involved were evaluated. Specifically, while optimizing the operating conditions of the SOEC system, it was assessed that how the annual production (the number of units), lifetime, operation rate, and electricity cost of the SOEC module affect the hydrogen production cost under the SOEC system. Based on such assessments, the construction cost of a renewable hydrogen station for fuel cell vehicles (FCVs) was assessed, and then, the hydrogen production cost that included this construction cost was assessed. As a result, the following two facts were found. (1) If the electricity cost remains within the 15-2.5 JPY/kWh range, the hydrogen production cost will range from 120 to 37 JPY/Nm³-H₂, depending on the operation rate. (2) Reducing the hydrogen production cost to a level equivalent to the gasoline sales price (40 JPY/Nm³-H₂) will require downsizing the unit and redesigning the pressurization and storage processes.

Proposals for Policy Development

- Reducing the size and cost of equipment: Size and cost reduction of the hydrogen production module, compressor, and accumulator is vital to promote the development of hydrogen stations because it greatly affects the station installation cost.
- Redesigning the pressurization and storage processes: Lowering the pressure for the accumulator (high-pressure tank) will make it possible to reduce the costs of the accumulator and the compressor. For the longer term, efforts should be made to reduce the hydrogen production cost to 40 JPY/Nm³-H₂, a level comparable to the current gasoline price. Two processes may be viable to attain this goal. One is to reduce the cost of the compressor by taking advantage of electrochemical pressurization that is made possible by adopting, for an electrolysis cell, a fuel cell that uses a proton-conductive electrolyte membrane [1]. The other is to chemically convert hydrogen into ammonia or other energy carriers for transport and storage before using it for power generation[2].

1. Designing a Steam Electrolysis (SOEC) System and Optimizing Its Operating Conditions

An SOEC system was designed, and its operating conditions were optimized while taking the thermo-neutral point into account. As a result, it was found that the hydrogen production efficiency was 83%, or even considering the process of increasing pressure to 80 Mpa, it was 76%. The hydrogen production rate was 300.8 Nm³/h, almost equivalent to the standard production level for commercial hydrogen stations (300 Nm³/h).

2. Assessing the SOEC System Cost and the Hydrogen Production Cost

The SOEC system cost was assessed based on two assumptions: (i) The lifetime of the SOEC module will be extended to three years; and (ii) the lifetime of BOS (Balance of system) will be 15 years.

It was found that the SOEC module cost will be largely halved if the annual production is increased from 100 units to 1,000 units, and, in addition to the SOEC module cost, costs for compressor and accumulator account for a large part of the system cost.

Based on these findings, the assessment showed that in order to reduce the hydrogen production cost, to a level equivalent to the gasoline sales price in terms of combustion heat (40 JPY/Nm³-H₂), conditions of the level of an electricity cost of 5 JPY/kWh, an operation rate of 30% or more, and at least a 3-year lifetime of the SOEC module (Figure 1) are required.

3. Evaluating Hydrogen Stations for Fuel Cell Vehicles (FCVs)

It was suggested that the construction cost of an on-site renewable hydrogen station, based on a SOEC system (with the hydrogen production unit installed on the site) (Figure 2), can be reduced to 400 million JPY or less by setting the lifetime of the SOEC module to three years or more (Figure 3).

If the construction cost of hydrogen stations are included, the hydrogen production cost on the condition that the electricity cost is in the 15-2.5 JPY/kWh range will be 120-70 JPY/Nm³-H₂ at an operation rate of 33% (or 8h/day) and 86-37 JPY/Nm³-H₂ at an operation rate of 90%.

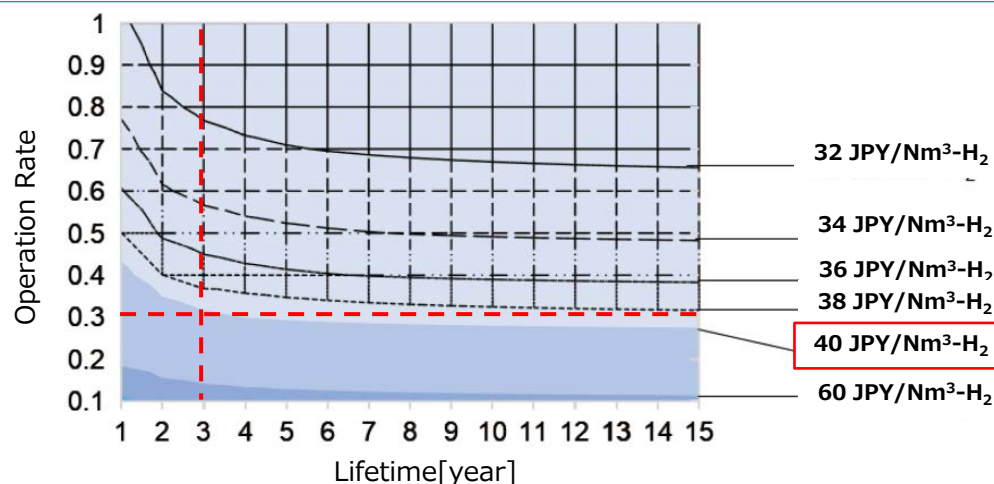


Figure 1 How the Hydrogen Production Cost Depends on the Operation Rate and the Lifetime of the SOEC Module (Electricity Cost: 5 JPY/kWh)

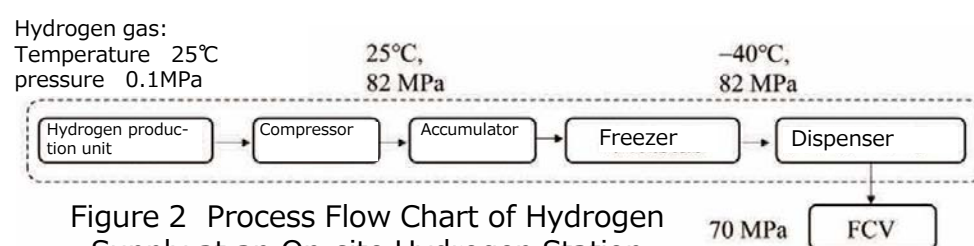


Figure 2 Process Flow Chart of Hydrogen Supply at an On-site Hydrogen Station

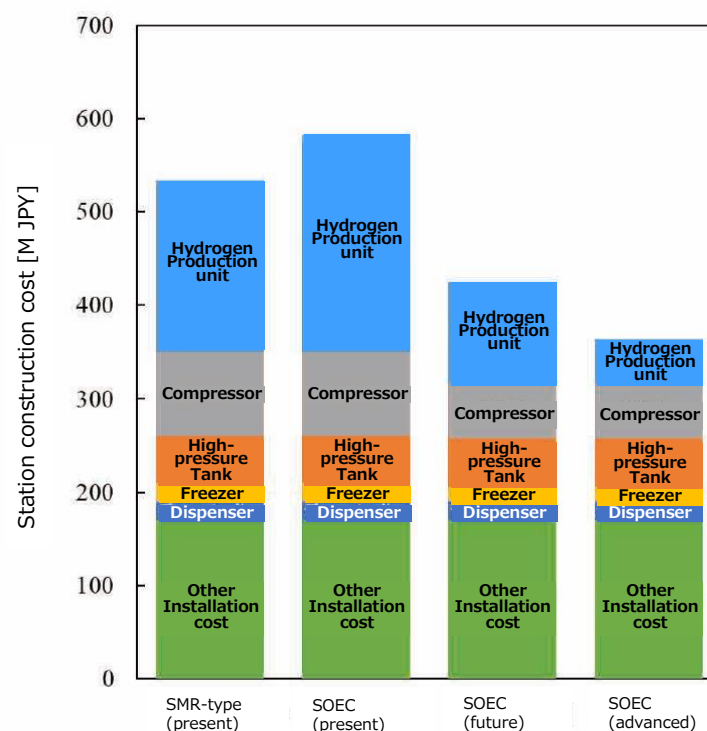


Figure 3 Construction Cost Structure of a Hydrogen Station (300 Nm³/h) (SMR (present), SOEC (present): A 1-year lifetime of the module and an annual production of 100 units; SOEC (future): A 1-year lifetime of the module and an annual production of 1,000 units); and SOEC (advanced): A 3-year lifetime of the module and an annual production of 1,000 units)

<https://www.jst.go.jp/lcs/pdf/fy2020-pp-02.pdf>

[1] Smart Hydrogen Station (SHS) developed by Honda Motor Co., Ltd. <https://global.honda/innovation/FuelCell/smart-hydrogen-station-engineer-talk.html>.

[2] Kojima, Yoshitsugu, ed. Hydrogen Energy System Using Ammonia, CMC Publishing, p239, June 2015.

Impact of Progress of Information Society on Energy Consumption (Vol. 2): Current Status and Future Forecast of Data Center Energy Consumption and Technical Issues

Summary

It is pointed out that the development of the information society may bring a huge increase in power consumption. This study focused on data center among the major ICT infrastructures, examined what kind of equipment contributed to the increase in power consumption, and estimated the total power consumption of data centers on the assumption that current technology will remain in place. Some of its findings are as follows: (i) servers account for a large portion of the power consumption; (ii) the power consumption of the AI task such as deep learning will increase more rapidly; and (iii) total power consumption both in Japan and worldwide is expected to surge toward 2030 and yet further toward 2050. Finally, the study identifies some of the challenges in reducing power consumption. These challenges are summarized as targets for power efficiency and power consumption reduction for each component devices.

Proposals for Policy Development

- Although the computational load of data centers is likely to continue to soar, the ongoing global shift in the energy portfolio toward low-carbon energy means that it is difficult to expect a significant increase in power supply. In order to provide the services necessary for a low-carbon society, it is necessary to promote energy saving in data centers.
- Power demand for 2030 and 2050 is estimated on the assumption that the latest equipment currently available is used. CPUs and GPUs have the greatest potential to reduce power consumption. The target should be to increase the power efficiency of these two kinds of devices by 3-10 times the current level by 2030 in terms of Gflops/W and some 1,000 times as much by 2050. The target for memory, power supply, and storage systems should be to reduce their power consumption to 1/10 in 2030 and 1/1000 in 2050.

1. Breakdown of Power Consumption

The main IT equipment of the data center is servers, storages, and network switches, as well as the power supply systems (transformers, converters, inverters, uninterruptible power supplies (UPSs), etc.) and the air-conditioning system (Figure 1). The total power consumption of data centers was calculated by adding up the estimated power consumption of each type of equipment.

In estimating the power consumption of servers, a distinction was made between (i) *basic tasks* – the portion where power consumption is proportional to conventional IP traffic, which includes Web services, search services, and e-mail services; and (ii) *AI tasks* – the portion that generates operations on a large scale, which is typified by deep learning.

The air-conditioning system and the power supply system were included in the process of calculating PUE (power usage effectiveness: the ratio between the total power consumption of data centers and the power consumption of IT equipment).

2. Future Projections of Data Center Power Consumption

The total power consumption of data centers for Japan and worldwide was estimated for 2018, 2030, and 2050 (Table 1).

- Total power consumption in 2018 was estimated 14 TWh for Japan and 190 TWh worldwide.
- If the latest equipment currently available is used (technological advancements are not factored in), total power consumption is projected as follows.

Japan: 90 TWh in 2030; 12,000 TWh in 2050

Worldwide: 3,000 TWh in 2030; 500,000 TWh in 2050

3. Challenges in Reducing Power Consumption

The breakdown of data center power consumption is currently 50% for servers, 25 to 30% for power supply and cooling systems, and 10% for storage. Servers are expected to make up 60-80% in the future, pointing to the utmost importance of reducing their power consumption. Specific types of equipment for servers that need energy saving include CPUs, storages, memories, and power supply units (inverters and converters). Power saving is especially important for CPUs and GPUs, both of which will likely face a remarkable increase in an AI task.

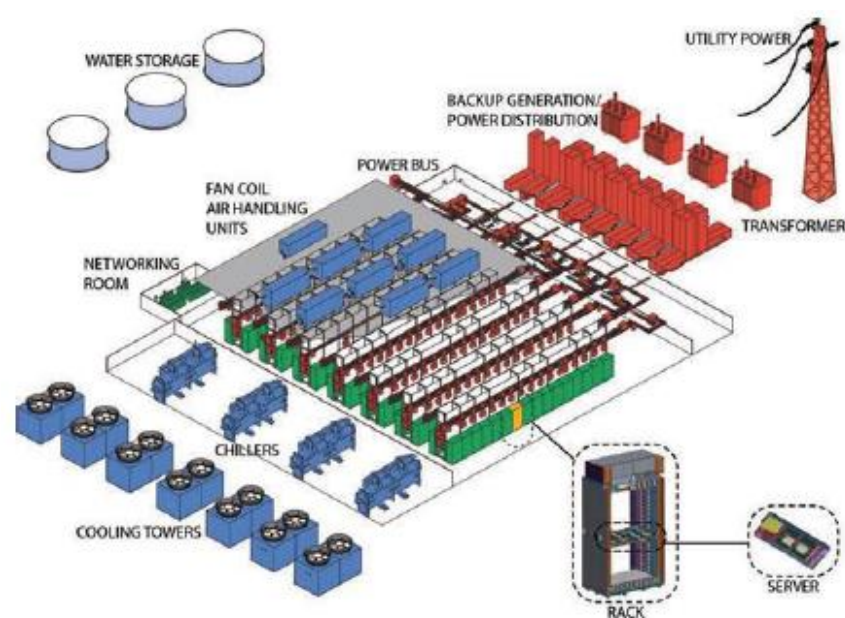


Figure 1: Data Center Layout[1]

Table 1: Current Power Consumption of Data Center and Future Projections

		domestic			global		
		2018	2030	2050	2018	2030	2050
IP traffic	ZB	0.7	11	1,400	11	170	20,200
power consumptions of data centers	TWh	14	90	12,000	190	3,000	504,000
power consumptions of server	basic task	TWh	6	30	3,500	90	450
	AI task	TWh	0.7	16	3,000	23	1,740
	total	TWh	7	46	6,500	113	2,190
CPUs	basic task	TWh	4	20	2,200	60	280
	AI task	TWh	0.5	12	2,300	17	1,320
	total	TWh	4	32	4,500	77	284,000
memories	basic task	TWh	1	7	890	16	110
	AI task	TWh	0.1	2	340	3	190
	total	TWh	1	9	1,230	19	300
power supply etc	basic task	TWh	1	3	410	14	60
	AI task	TWh	0.1	2	400	3	230
	total	TWh	1	5	810	17	290
power consumptions of storages	TWh	2	29	3,700	27	430	
power consumptions of switches	TWh	0.1	1	70	2	20	
power supply, cooling, etc	TWh	5	11	1,500	43	400	

[1] L. A. Barroso, et al., "The Datacenter as a Computer: Designing Warehouse-Scale Machines, 3rd ed.," Morgan & Claypool Publishers (2018).

Impact of Progress of Information Society on Energy Consumption (Vol. 3): Current Status and Future Forecast of Network-Related Energy Consumption and Technical Issues

Summary

The power consumption of the network was estimated in relation to the progress of information society on the assumption such as a core, metro, and access network structure, and the issues were examined. Assuming both an annual increase of 27% in traffic and a fixed state-of-the-art technology level, the problem to be considered is the increase of the power consumption of access systems that account for 80% of the total, especially wireless access systems in them. The paper also compared the future increase in power consumption of telecommunications networks with that of data centers, which also constitute a key part of ICT infrastructure. The finding is that they are almost on the same level.

Proposals for Policy Development

- As far as the telecommunication network sector is concerned, a sharp rise in power consumption is expected for access networks, especially wireless access systems. The equipment in question will be wireless base stations and routers. Research to reduce such power consumption is particularly important. The reduction target should be set at a half or one third of the current levels in 2030 and further one hundredth or less in 2050.
- In telecommunication networks it is important to consider not only hardware but also communication systems and architectures, in order to reduce power consumption in facilities with low traffic volume while coping with peak traffic.
- The types of hardware such as transmission amplifiers at base stations, routing-related processors, and switches are listed as devices of high-power consumption. It is important to save energy in these devices.

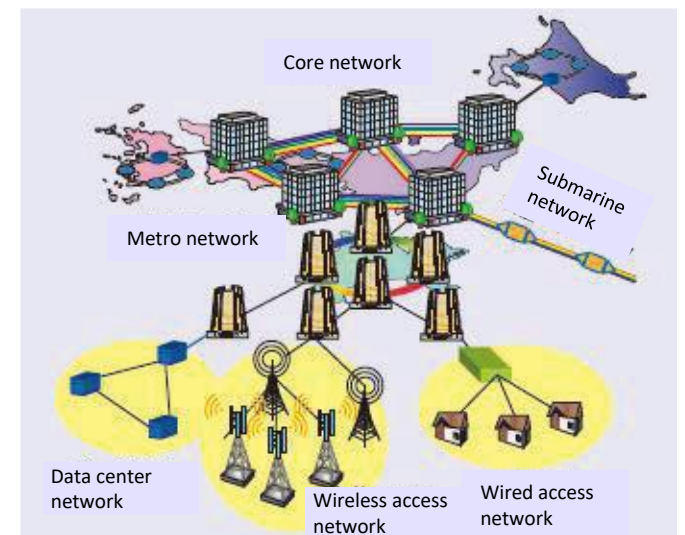


Figure 1: Network Structure[2]

1. Network Structure

The telecommunication network is classified into the core, metro, and (wired and wireless) access networks (Figure 1). The main equipment and facilities are routers in the core and metro networks, and base stations in the access networks.

2. Calculation of Network Power Consumption

The power consumption of the entire network was estimated to be 23 TWh in Japan and 490 TWh worldwide in 2018.

Assuming both an annual increase of 27% in traffic and a fixed state-of-the-art technology level, traffic volume for 2030 and 2050 was estimated. The estimated power consumption of the main equipment of each network was added up, and current and future total power consumption for Japan (the bottom row of Table 1) and worldwide (the bottom row of Table 2) was estimated.

Japan: 93 TWh in 2030; 9,000 TWh in 2050

Worldwide: 2,400 TWh in 2030; 260,000 TWh in 2050

Access networks account for 80% of the total and are expected to increase further with the expansion of applications.

3. Challenges in Reducing Power Consumption

The types of equipment that use the largest amount of energy are wireless base stations, followed by routers. The challenge for saving energy consumption lies in improving the efficiency of power amplifiers for wireless base stations and processors for routers.

4. Comparison in Power Consumption between Data Centers and Networks

Comparing the power consumption of the data center [1] and the network, which are the main ICT infrastructures, it was found that both were almost at the same levels (Tables 1 and 2).

Table 1: Current Power Consumption of ICT Infrastructure in Japan and Future Projections

Domestic		2018	2030	2050
Datacenter		TWh/Y	TWh/Y	TWh/Y
	server	7	62	9,600
	storage	2	29	3,700
	switch	0.1	1	70
	power supply	5	13	2,000
	Total	14	90	12,000
Network				
	Core	1	2	231
	Metro	4	13	1,510
	Access	18	78	7,000
	Total	23	93	9,000

Table 2: Current Power Consumption of ICT Infrastructure Worldwide and Future Projections

Global		2018	2030	2050
Datacenter		TWh/Y	TWh/Y	TWh/Y
	server	113	2,190	384,000
	storage	27	430	51,000
	switch	2	20	3,400
	power supply	43	400	66,000
	Total	190	3,000	500,000
Network				
	Core	25	42	4,900
	Metro	90	260	31,400
	Access	370	2,100	220,000
	Total	490	2,400	260,000

[1] LCS, "Impact of Progress of Information Society on Energy Consumption (Vol. 2): Current Status and Future Forecast of Data Center Energy Consumption and Technical Issues", Proposal Paper for Policy Making and Governmental Action toward Low Carbon Societies, February 2021.

[2] Miyamoto, Yutaka, et al. "Ultrahigh-speed Transmission Technology for Future High-capacity Transport Networks," *NTT Technical Review*. Vol. 17, No. 5. May 2019.

Methane Production from Biomass Wastes by Anaerobic Fermentation (Vol. 5) : Feasibility Study of Biological Hydrogen Methanation Process

Summary

A study was made on the issues of biological hydrogen methanation, which is the production of methane, using methane, carbon dioxide, and hydrogen that are generated in the methane fermentation process of waste biomass, and also hydrogen generated from electrolysis of water and other processes for making up the deficient of hydrogen. The cost of producing methane using this process is 6.9 JPY/MJ, which is slightly more expensive than the current gas rate of 3.5 JPY/MJ plus the DAC cost, which is 5.7 JPY/MJ, but given the benefit of treating waste biomass, biological hydrogen methanation is worthwhile. Studies on fermenter components and system optimization will be needed.

Proposals for Policy Development

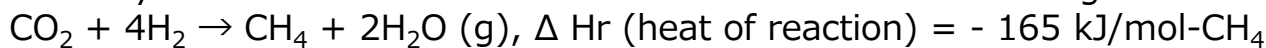
- Biological hydrogen methanation has not yet been fully developed in Japan. It is necessary to promote the elucidation of the fermentation mechanism of fermenting bacteria, the development of reaction engineering that accelerates the dissolution of hydrogen, and the effective utilization of waste biomass.
- For methane fermentation, analysis using the fermentation model used in this study will be beneficial for studying the rationalization of the process, leading to the prediction of the fermentation system. It is important to study the fermentation model and spread this process to be widely used.

1. Methane fermentation model

The fermentation pathways via ethanol [2] and lactic acid [3], which are important in hydrogen fermentation, were added to the ADM1 model [1] that has been used as a base. As a result of streamlining the process and predicting the fermentation system, the amount of methane and hydrogen produced were able to be determined when conditions such as initial NH₄ concentration and temperature were changed. These results can be used to study the conditions for methane and hydrogen production by biomass fermentation.

2. Investigation of biological hydrogen methanation ([4], [5])

The cost and amount of methane produced by the fermentation-methanization process using CO₂, H₂, and CH₄ produced by methane fermentation of biomass wastes were investigated. The reaction equation is as follows:



Two types of systems were studied: (Case 1) a two-stage system consisting of a hydrogen fermentation tank and a methane fermentation tank, and (Case 2) a system in which the hydrogen fermentation tank was removed for simplification and both raw garbage and sewage sludge were fed into the methane fermentation tank.

3. Studied model and cost of methane gas

A model of methane gas production by methane fermentation from waste biomass (sewage sludge and food waste) and biological hydrogen methanation was studied for a city with a population of 100,000.

The process flow for Case 1 is shown in Fig. 1.

The amount of methane produced is calculated to be 97 m³/h (95% methane), which can replace 9% of the gas energy consumed by a city of the same size. Methane gas is easier to use for consumer purposes than hydrogen, including safety aspects.

The methane production cost was calculated from fixed costs such as the construction and operating costs of the model, and variable costs such as electricity and supplied hydrogen (Table 1). However, if fossil fuel-derived methane is used, the CO₂ generated must be captured by DAC in a zero-carbon society. This will cost 2.2 JPY/MJ, which together with the current gas price of 3.5 JPY/MJ, will result in a cost of 5.7 JPY/MJ. The costs of methane production for the entire process is 7.0 JPY/MJ for Case 1 (with hydrogen fermentation) and 6.9 JPY/MJ for Case 2 (without hydrogen fermentation), which is a little more expensive than that of fossil fuel-derived methane. Considering the benefit of treating the waste, this reaction system is worthwhile.

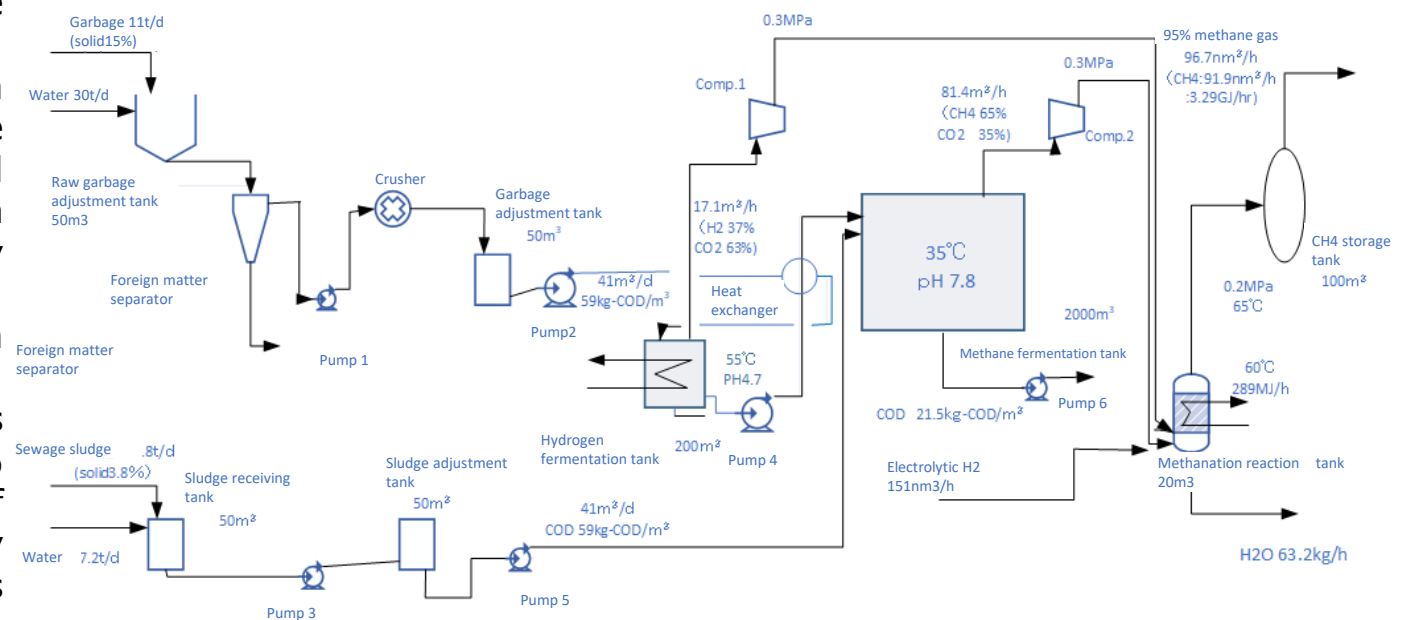


Fig. 1. Flow chart of the bio-methanization process

Table 1. Methane production cost
Methane production rate: 91 Nm³/h, 3.26GJ/h(26.1 TJ/y)

CH ₄ production cost					
	Case 1		Case 2		Remarks
Fixed cost		Fixed cost burden		Fixed cost burden	
Construction cost	453million JPY	68million JPY	396million JPY	59million JPYy	Annual expense ratio 15%
Operating costs	9 people	45million JPY/y	9 people	45million JPY/y	5 million JPY/ person/ year
Total		4.3JPY/MJ		4.0JPY/MJ	
Variable cost	Specific "energy" or "material" consumption	Cost (JPY/MJ)	Specific "energy" or "material" consumption	Cost (JPY/MJ)	Unit price, etc.
Electric power	40.5 kWh/GJ	0.481	34.7 kWh/GJ	0.416	12JPY/ kWh
Sewage Sludge	0.305 t/GJ	0	Same as left	0	
Garbage	0.100 t/GJ	0	Same as left	0	
Hydrogen	46.3Nm ³ /GJ	2.29	50.0Nm ³ /GJ	2.5	50JPY/Nm ³
Generated heat(60°C)	88.6MJ/GJ	Δ0.104	Same as left	Δ0.104	1.17JPY/MJ(=1.5JPY/MJ×333/423)
nutrient	Ammonium phosphate 0.129kg/GJ KC I 0.073 g/GJ	0.021	Same as left	0.021	Produced water: 19.2kg/GJ Ammonium phosphate: 140JPY/kg, KCl: 45JPY/kg
Total variable cost		2.7JPY/MJ		2.9JPY/MJ	
CH₄ Production cost		7.0JPY/MJ		6.9JPY/MJ	

[1] D.J. Batstone, et.al, 'Anaerobic Digestion Model No. 1', Scientific and Technical Report No. 13, IWA publishing, 2002.
 [2] E.Shi, J.Li, and M.Zhang, Water Res., 161 (2019) 242-250.
 [3] G.Antonopoulou, et. al, Int. J. Hydrogen Energy, 37 (2012) 191-208.
 [4] B. Lecker et al. Bioresource Tech., 245 (2017) 1220-1228.
 [5] D. Rusmanis et al, Bioengineered, 10 (2019) 604-634.

Cost Evaluation of Direct Air Capture (DAC) Process (Vol. 2) : Adsorption Method

Summary

The costs and issues of DAC processes using amine / nanofiber systems and MOFs-74 (Metal-Organic Frameworks) systems were investigated. The amine/nanofiber system has low adsorptivity and high airflow resistance of the adsorbent [1]. The energy cost was higher, and the DAC cost for the assumed case was 117 JPY/kg-CO₂. The energy cost of MOFs system which assumes a honeycomb structure is low due to a lower air-flow resistance than the amine/nanofiber system. However, because the price of MOF as an adsorbent is high, it is necessary to double the life of the adsorbent (four years) at least. The DAC cost is estimated at 71 JPY/kg-CO₂ and verification is needed for such estimation in the future. In the case of the KOH-CaCO₃ alkali absorption method studied so far, the DAC cost is estimated at 35 JPY/kg-CO₂ [2]. This is a promising process at the moment though there is a challenge to prove whether the cost can be lower.

Proposals for Policy Development

- It is necessary to develop technology to reduce the cost of DAC to less than 35 JPY/kg, or preferably less than 20 JPY/kg-CO₂.
- The alkali absorption method, the NFC-amine adsorption method, and the MOFs adsorption method have many issues to be demonstrated and developed. Thus, all these methods need to be developed with clear goals.
- In order to develop optimal adsorbents, the results obtained by making full use of computational chemistry and other methods need to be applied to specific developments for efficient studies.

1. Evaluation and cost of amine/nanofiber system

A fiber filter formed by impregnating nanofibers (NFC) with amine (H₂N(CH₂)₂NH(CH₂)₃SiCH₃(OCH₃)₂: AEAPDMS) was used as an adsorbent.

(1) Evaluation of CO₂ adsorptivity of AEAPDMS

In order to evaluate the heat of adsorption by understanding the mechanism by which AEAPDMS adsorbs CO₂, quantum chemical calculations were performed, and the change in adsorptivity due to the change in electronic state in the presence or absence of water, the ease of adsorption, and the heat of adsorption were estimated.

Quantum chemistry provides a powerful tool for improving the efficiency of technology development in this field (Fig. 1. Example of molecular structure).

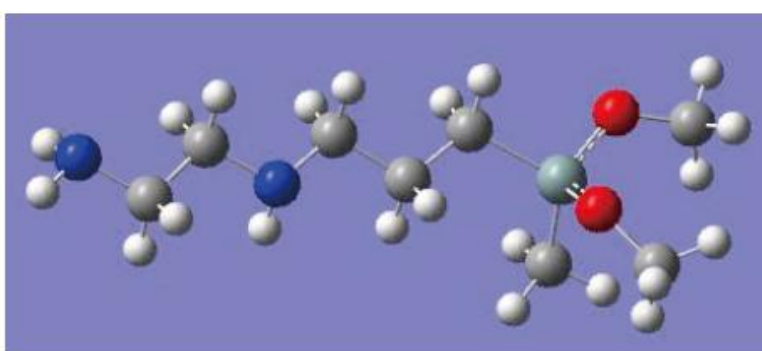


Fig. 1. Example of the molecular structure of AEAPDMS

(2) Study using assumed process

In the assumed process for examining performance and cost, the CO₂ concentration in the air was set to 400 ppm, the CO₂ capture rate to 112 t/h, and the CO₂ concentration at the outlet of the adsorption bed to 0 ppm. Assuming an adsorption rate of 0.5 mol/kg/h, the adsorption and desorption cycles were 60 minutes each, resulting in a DAC cost of 117 JPY/kg-CO₂ (Table 1).

2. Evaluation of MOFs-74 (Metal-Organic Frameworks) system and DAC cost

MOFs (Metal Organic Frameworks) are hybrid materials synthesized by the self-assembly of metals and organic ligands. It has also been investigated for the adsorption of CO₂, and it has been confirmed that Mg-MOF-74 has a large adsorption capacity, but the development is currently in the laboratory stage. Assuming a honeycomb structure as the adsorption layer, the cost was calculated as in 1. (2), and it was 71JPY/ kg-CO₂ (Table 1).

3. Discussion and issues

In addition to the NFC-amine and MOFs methods, the costs of the KOH-CaCO₃ alkaline method and the amine absorption method for coal boiler flue gas were compared (Table 1). The first three methods are DAC and have an inlet CO₂ concentration of 400 ppm. The last method, amine absorption, has an inlet CO₂ concentration of 14.3%.

Table 1. Comparison of CO₂ capture costs (CO₂ capture rate 112t/h)

Process	DAC		DAC	Coal boiler flue gas	Remarks		
	NFC-amine method	MOFs Method	Alkali method	Amine absorption			
			CO ₂ 400ppm→110ppm	CO ₂ 14.3%→1.56%			
Fixed cost (JPY/kg-CO ₂)	51.9	26.7	20.7	3.6*	*Capacity is corrected to 112 t/h		
Variable cost (JPY/kg-CO ₂)	65.0	44.4	14.7	5.9			
Electric Power	4.14 k Wh/kg	49.7	1.6kWh/kg	19.2	0.14kWh/kg	1.7	12JPY/kWh
Heat				8.84MJ/kg	12.5MJ/kg	3.8	1.5JPY/MJ
Absorbent	15.3	25.2	1.4			0.2	
Other						0.2	
Total (JPY/kg-CO₂)	116.9	71.1	35.4	9.5			

The theoretical energy required to separate CO₂ for DAC was four times higher than for boiler flue gas, resulting in a higher DAC cost by adsorption methods (NFC-amine and MOFs methods). The features of each process are as follows: (1) In the case of CO₂ capture from boiler flue gas, the capture efficiency is 90% and the cost is less than 10 JPY/kg, but the outlet cannot be zero carbon because of the absorption method. (2) In the case of DAC, the inlet concentration of CO₂ is as low as 400 ppm, and the capture cost is about 35 JPY/kg for the alkaline method (outlet CO₂ concentration: 110 ppm) [2]. In places like the U.S., where LNG is inexpensive (0.35 JPY/MJ), the price is about 25 JPY/kg-CO₂. This method has its challenges, but it is a promising process. (3) The NFC-amine method has high costs of equipment and power due to a high air-flow resistance of the adsorbent, and the current cost is over 100 JPY/kg. (4) The MOFs method has a lower air-flow resistance and power cost, so it could be less than 100 JPY/kg, but experimental proof is required. In order to reduce the cost of DAC to less than 35 JPY/kg, or preferably less than half, there are many issues that need to be resolved, and it is necessary to proceed with demonstration experiments such as improving the performance of the adsorbent, extending its life, and reducing its ventilation resistance.

[1] Jan Wurzbacher, "Capturing CO₂ from Air," Herbstworkshop Energiespeichersysteme, TU Dresden, 9 November 2017.

[2] LCS, Proposal Papers for Innovation Policy Development, "Cost Evaluation of the Process of Direct Air Capture (DAC) Process of Carbon Dioxide," February 2020.

Technical Challenges and Forecasts on Safety Assessment of Large-Scale Energy Storage Systems for Its Social Implementation

Summary

The aim of this paper is to review previous studies of the safety and risk of large-scale energy storage systems and present critical concepts and approaches required in the future for the systems. Firstly, technological trends in the safety assessment of systems were surveyed, and then as a framework for the sake of organizing the results of the survey, methods of identification of risk scenarios, risk analysis, and risk assessment are presented. For instance, critical risk items related to the safety of large-scale storage battery systems were identified by way of risk analysis, and a trial risk modeling for risk quantification was carried out. Necessary elements for the safety assessment of large-scale energy storage systems are presented as proposals.

Proposals for Policy Development

- In implementing large-scale energy storage systems in society, it is necessary to identify relevant risks to be addressed by taking into account altogether the economy and safety, and then to share the risks among parties concerned. In addition, it is important for persons in charge of policy planning to coordinate and encourage discussion on the risks, which parties concerned with the system consider important.
- It is important to establish safety standards of large-scale energy storage systems. If taking the initiative in the establishment of safety standards for quantitative assessment of safety as well as safety technology related to the systems is successful, attaining an internationally advantageous position may become possible.
- Various kinds of operation statistical data are needed in the risk assessment, but they are currently confidential information. It is necessary to build a data-sharing environment available for risk assessment personnel by creating a relevant database.

1. Trends in safety technology

The trends in research concerning the safety of lithium-ion batteries (hereafter referred to as LiB) used for large-scale energy storage systems were explored through a literature database survey, and LiB accident factors and classification of safety measures were summarized. The survey revealed that the research on LiB safety to date was mainly targeted on the danger of storage batteries and safety measures against the danger. In 2020, a technical document concerning whole system consideration of large-scale storage battery systems was published [2] overseas, and the relevant research will probably be progressively promoted.

2. Identification of risk scenarios

A “Bow-Tie” analysis model which summarizes event progression after an accident of large-scale storage battery system and safety measures preventing the event progression on either side of LiB thermal runaway accident (Fig. 1), was used to ascertain the vulnerability of the accident scenario or the system. It is important to identify the risk scenarios, presented on the left side, caused by accident factors, and the scenarios, presented on the right side, affecting the whole system or society after the occurrence of LiB thermal runaway. Then, overall risks were identified by applying HAZOP, which is an analysis method for identifying an accident scenario by way of a combination of parameters, such as temperature, and guide words. For instance, a scenario of “propagation of thermal runaway of a single cell caused by inner short-circuit to adjacent cells in a chain reaction fashion,” etc. were identified (Table 1).

3. Risk analysis and assessment

An initial investigation for the preparation of quantitative risk analysis was carried out by building a model of physical phenomena of the risk scenario identified above. The risk scenario was analyzed by means of the model of physical phenomena and Monte Carlo simulation on the condition that when the cell temperature exceeds the threshold, thermal runaway will be triggered. In this way, calculation of the thermal runaway probability of each cell of a storage battery module became possible, but refinement of the simulation result needs measurement values of input parameters. More accurate estimations may become possible by building a database of parameters.

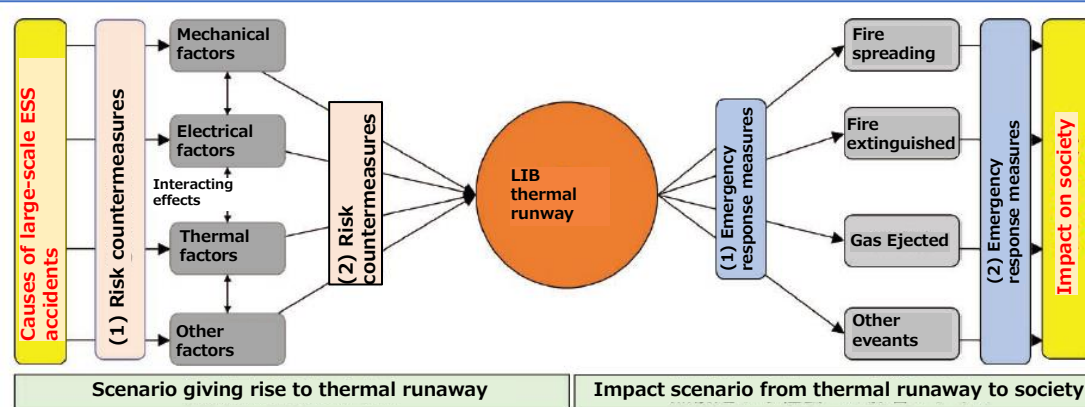


Fig. 1. A Bow-Tie Analysis Model Suggested for Thermal Runaway Accident of Large-Scale Storage Battery System

Table 1. Examples of Risk Scenarios Identified by Means of HAZOP

ESS model	Parameter	Guide word	Meaning	Causes	Effects within single cell	Effects on adjacent cells	Effects on the module	Effects on the whole system
Battery board	Temperature	MORE	Cell temperature elevated	<ul style="list-style-type: none"> High temperature External Fire Poor cooling Electrolyte reaction 	<ul style="list-style-type: none"> (1) Elevated cell temperature resulting in disintegration of electrode, electrolyte, and separator. (2) Separator damaged, leading to inner short-circuit state and heat generation (3) Cell temperature further elevated, leading to disintegration of electrode and electrolyte (4) Cell thermal runaway 	<ul style="list-style-type: none"> (1) Cell thermal runaway causing the temperature of adjacent cells to rise (2) Elevated cell temperature resulting in disintegration of electrode, electrolyte, and separator (3) Separator damaged, leading to inner short-circuit state and heat generation (4) Cell temperature further elevated, leading to disintegration of electrode and electrolyte (5) Cell thermal runaway 	<ul style="list-style-type: none"> (1) Thermal runaway of adjacent cells, leading to the elevation of temperature of other cells and the whole module (2) Disintegration of electrode, electrolyte, and separator within the cells of the module (3) Inner short-circuit state and heat generation within the cells of the module, resulting in ignition and fire of the module 	<ul style="list-style-type: none"> (1) Fire in the module spreading to the battery board (2) Fire spreading to the whole system, resulting in large-scale fire

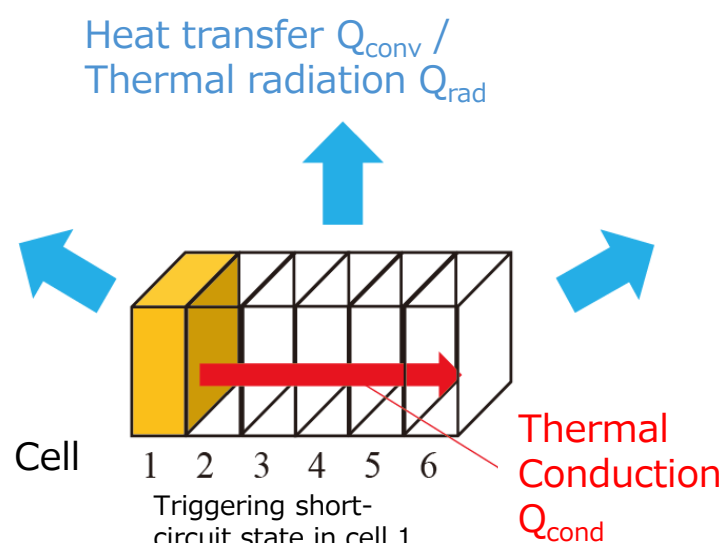


Fig. 1. Conceptual Experiment Apparatus Diagram of Previous Research [1]

[1] Feng X, Lu L, Ouyang M, Li J, He X, “A 3D thermal runaway propagation model for a large format lithium-ion battery module,” Energy 2016;115:194-208.

[2] International Electrotechnical Commission (IEC), IEC 62933-5-2, “Electrical energy storage (EES) systems – Part 5-2: Safety requirements for grid-integrated EES systems – Electrochemical-based systems,” 2020.

Secondary Battery System (Vol. 9) : Cost Evaluation of a Lithium-ion Battery Using Next-Generation Electrode Active Material

Summary

An attempt was made to predict future changes to higher specific energy and lower costs of lithium-ion batteries (LIBs) by calculating the manufacturing costs of LIBs while taking into account recent technological levels. Incorporation of next-generation electrode active material into LIBs was designed, and the manufacturing cost of a LIB was estimated. While the manufacturing cost of the current model (year 2020) is from 11.9 to 23.2 JPY/Wh, it was found in the estimation that the manufacturing cost of the future model may be reduced to 5.1 JPY/Wh at the lowest. On the other hand, to accomplish the short-term targets of energy density (500 Wh/kg or more) and manufacturing cost (10,000 JPY/kWh per battery pack) for EV applications, etc. by 2030, about ten years of development period remain, and therefore research for that end should be encouraged and promoted.

Proposals for Policy Development

- As specific measures for attaining high-performance low-cost secondary batteries, a proposal was made to replace the current positive and negative electrodes with a next-generation positive-electrode active material and a Si negative electrode, respectively, or alternatively with S positive-electrode active material and a metal Li negative electrode, respectively. It was shown in a quantitative manner that the replacement of these electrodes is technically feasible.
- With the technology development and implementation under current development investment, it is predicted to be able to accomplish the targets after 2040. To accomplish new targets in the future, it is essential to make urgent, concentrated investment in terms of equipment, budget, and human resources through close cooperation between industry, academia, and government.

1. Secondary battery design specifications for evaluation

The structure of the secondary battery for evaluation was such that a stacked cell, in which several single cells were stacked, was sealed by the enclosure of a pouch material (Fig. 1). Dimensions were selected by referring to LIBs on the market. Table 1 shows the configuration of electrode active material and the battery voltage. In the case of References 1 through 4, electrode active materials (conventional materials) used in LIBs on the market were employed. In the case of Examinations 1 through 9, materials other than conventional materials were employed for one or both of positive and negative electrode active material ([1] - [5]).

2. Estimated manufacturing cost

Fig. 2 shows the estimated manufacturing cost and energy density of secondary batteries for evaluation batteries (References 1 through 4 and Examinations 1 through 9 in Table 1) for several groups classified by combination of different electrodes.

3. Future prospects

To reduce the manufacturing cost and to improve the energy density, it will be necessary to replace positive and negative electrodes with next-generation electrode active materials.

For the estimation of the energy density and the manufacturing cost, the following settings were assumed: For the short-term targets (from year 2030 to year 2040), replace either or both positive or negative electrode with next-generation positive-electrode active material and a Si negative electrode, respectively. For the medium-term targets (year 2050), replace positive and negative electrodes with next-generation positive-electrode active material and a Si negative electrode respectively, or alternatively with S positive-electrode active material and metal Li negative electrode, respectively. Specific energy and manufacturing cost were estimated by referring Fig. 2.

Current group (G1): 277 Wh/kg, 11.9 JPY/Wh

Short-term targets group (G2, G3, and G5):

300 Wh/kg or more, 11.6 JPY/Wh or less

Medium-term targets group (G4, G6, and G7):

300 Wh/kg or more, 10.0 JPY/Wh or less

Note, however, that it is estimated that more time will be needed for practical realization because both positive and negative electrodes should be changed to accomplish the medium-term targets (year 2050).

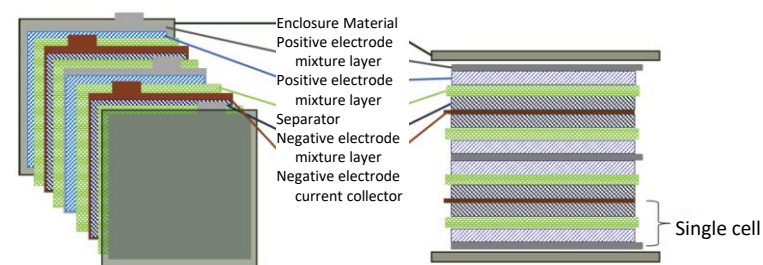


Fig. 1. Conceptual Configuration Diagram of Secondary Battery for Evaluation (Left: Exploded Perspective View, Right: Cross Section)

Table 1. Configuration of Electrode Active Material and Battery Voltage of Secondary Batteries for Evaluation

	Positive Electrode			Negative electrode			Battery voltage [V]
	Active material	Capacity [mAh/g]	Capacity utilization	Active material	Capacity [mAh/g]	Capacity utilization	
Reference 1	LiNi _{0.8} Co _{0.15} Al _{0.05} O ₂	196	0.72	C ₆	353	0.95	3.6
Reference 2	LiNi _{0.33} Mn _{0.33} Co _{0.33} O ₂	169	0.61	C ₆	353	0.95	3.6
Reference 3	LiFePO ₄	165	0.97	C ₆	353	0.95	3.3
Reference 4	LiMn ₂ O ₄	110	0.74	Li _{4/3} Ti _{5/3} O ₄	165	0.94	2.24
Examination 1	Li _{1/2} Ti _{0.4} Mn _{0.4} O ₂	300	0.76	C ₆	353	0.95	3.3
Examination 2	Li ₂ Mn _{1/2} Ti _{1/2} O ₂ F	320	0.70	C ₆	353	0.95	3.3
Examination 3	LiNi _{0.5} Mn _{1.5} O ₄	135	0.92	C ₆	353	0.85	4.55
Examination 4(a)/4(b)	LiNi _{0.8} Co _{0.15} Al _{0.05} O ₂	196	0.72	Si	1,007/4,197	0.24/1	3.3
Examination 5(a)/5(b)	LiNi _{0.33} Mn _{0.33} Co _{0.33} O ₂	169	0.61	Si	1,007/4,197	0.24/1	3.3
Examination 6(a)/6(b)	Li _{1/2} Ti _{0.4} Mn _{0.4} O ₂	300	0.76	Si	1,007/4,197	0.24/1	3.0
Examination 7(a)/7(b)	Li ₂ Mn _{1/2} Ti _{1/2} O ₂ F	320	0.70	Si	1,007/4,197	0.24/1	3.0
Examination 8(a)/8(b)	LiNi _{0.5} Mn _{1.5} O ₄	135	0.92	Si	1,007/4,197	0.24/1	4.25
Examination 9	S	1,508	0.9	Metal Li	2,895	0.75	2.15

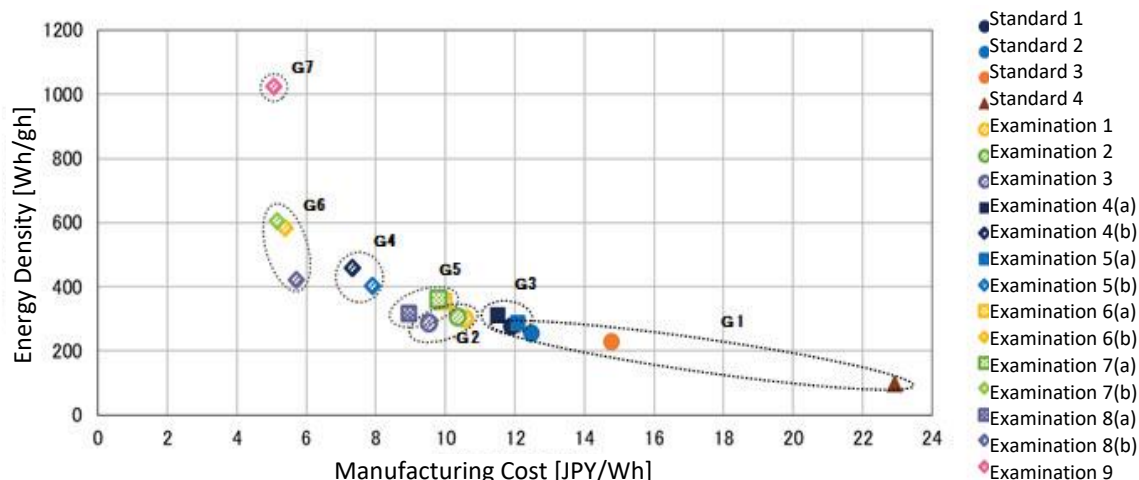


Fig. 2. Manufacturing Cost and Energy Density of Secondary Batteries for Evaluation (References 1 through 9 and Examinations 1 through 9) by Group Classification

- * Group classification into G1 through G7 (Table 1 classification in parentheses)
- G1: Conventional positive-electrode active material/ conventional graphite negative electrode (References 1 through 4)
- G2: Next-generation positive-electrode active material/ conventional graphite negative electrode (Examinations 1 through 3)
- G3 (future 2L): Conventional positive-electrode active material/ Si negative electrode (Examinations 4a and 5a)
- G4 (future 2H): Conventional positive-electrode active material/ Si negative electrode (Examinations 4b and 5b)
- G5 (future 3L): Next-generation positive-electrode active material/ Si negative electrode (Examinations 6a, 7a, and 8a)
- G6 (future 3H): Next-generation positive-electrode active material/ Si negative electrode (Examinations 6b, 7b, and 8b)
- G7 (future 4): S positive-electrode active material/ metal Li negative electrode (Examination 9)

[1] Naoaki Yabuuchi et al, "Origin of stabilization and destabilization in solid-state redox reaction of oxide ions for lithium-ion batteries," Nature Communications, vol. 7, no. 13814, 2016.

[2] Jinhyuk Lee et al., "Reversible Mn²⁺/Mn⁴⁺ double redox in lithium-excess cathode materials," Nature, vol. 556, pp. 185-190, 2018.

[3] "Development of Lithium-Ion Battery Active Material and Electrode Material Technology," Science & Technology Co., Ltd., pp. 42-52, 2014

[4] "Battery Handbook," Edited by the Committee of Battery Technology, the Electrochemical Society of Japan, Ohmsha, Ltd., p. 410-413, 201

[5] LCS, Proposals for Planning of Innovation Policy, "Secondary Battery System (Vol. 6)," February 2019 <https://www.jst.go.jp/lcs/pdf/fy2020-pp-08.pdf>

A Study on the Tele-communication Traffic Trends and the Impacts of Teleworking under Covid-19 State of Emergency

Summary

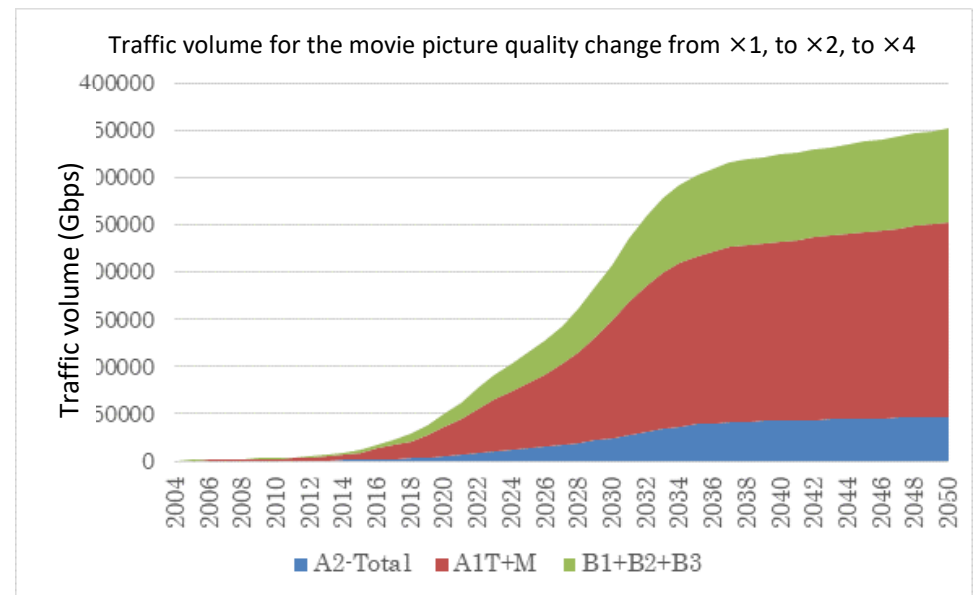
The role of ICT towards the building of a zero-carbon emission society is becoming important, but its progress will lead to a rapid increase in power consumption. However, data analysis from the standpoint of consumption regarding what kind of demand has brought about today's increase in the information traffic volume is limited. Therefore, in this proposal, existing statistical data regarding the increase in the tele-communication traffic demand were analyzed and examined. As a result, it was found that (1) the increase in the video streaming demand and the decrease in communications cost are significant factors for the increase in the tele-communication traffic volume; (2) productivity improvement due to the introduction of ICT is conspicuous in large enterprises; (3) although the tele-communication traffic volume has increased owing to teleworking more widely spreading under the declaration of a COVID-19 state of emergency, CO₂ emissions have fallen owing to a decrease in commuting by car.

Proposals for Policy Development

- Under the declaration of a COVID-19 state of emergency, differences have widened between job fields (enterprises, schools, etc.) where productivity has improved owing to the expanded introduction of ICT and job fields where productivity is not yet improved. To offer an incentive for introducing ICT to the job fields where ICT has not spread and to create a system consistent from resource procurement and the production site through sales management, as shown in Industry4.0, is an important government policy issue.
- The information traffic volume was largely increased following the introduction of teleworking through the utilization of ICT encouraged by the declaration of a COVID-19 state of emergency in 2020. It is expected that the change in ways of working involving a decrease in commuting hours may contribute to reductions in CO₂ emissions, helping the building of a "bright and affluent low-carbon society". Such social change due to the introduction of ICT may likely continue to the future, and development of information network infrastructure and measures responding to the increase in power demand associated with the development are required.

1. Information traffic analysis and prediction

The published data [1] was employed to estimate the growth rate of the information traffic volume; it was found that the yearly growth rate during 2004 through 2018 was 30.1%, and it increased rapidly especially during 2013 through 2018. Specific major factors were the increase in video streaming services and the decrease in communications cost. The information traffic demand was analyzed to estimate the traffic demand in the future. (Fig. 1). It was estimated that the demand may increase sharply toward 2030, but then saturate because of population decline toward 2050.



A1T+M: Fixed-line traffic of 5 ISP companies plus mobile communications traffic
 A2: Traffic by subscribers of other dedicated lines
 B1: Traffic exchanged at major IX in Japan
 B2: Traffic exchanged in Japan
 B3: Traffic exchanged overseas

Fig. 1 Estimation of tele-communication traffic volume in the future for the movie picture quality change from ×1, to ×2, to ×4

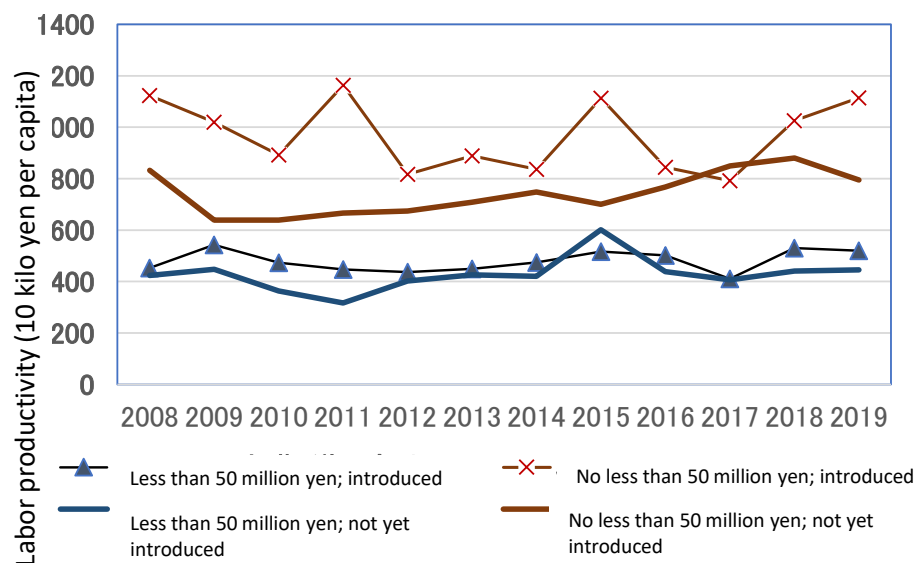


Fig. 2 Change over time in productivity owing to introduction of IoT by capital scale

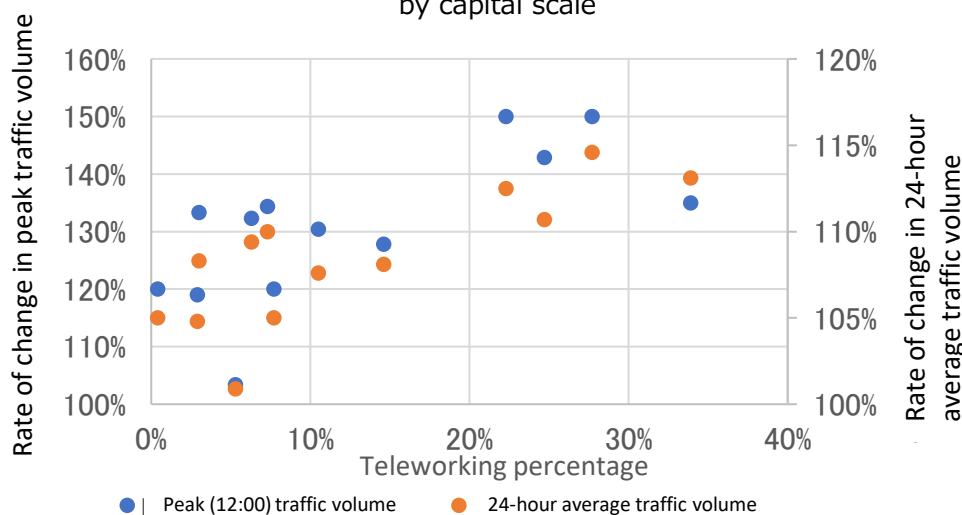


Fig. 3 Relationship between teleworking percentage and rate of increase in traffic volume

2. Impact of ICT on productivity

A questionnaire survey conducted by the Ministry of Internal Affairs and Communications [2] was used to summarize the adoption of the use of ICT and the impact on productivity. Fig. 2, "Change over time in productivity owing to introduction of IoT by capital scale," shows that productivity was improved owing to the introduction of IoT over the entire period. The estimated results can be interpreted to show that improvement of productivity by 20% to 30% may be possible for large enterprises with capital of no less than 50 million yen.

3. The impact of teleworking under a COVID-19 state of emergency

Under the COVID-19 crisis, teleworking has been attracting rapidly high attention, and many enterprises in urban areas adopted it. Analyzing one of the fact-finding surveys [3] and NTT's data of the change in traffic [4] found that a 10% increase in teleworking resulted in a 2.8% increase of the 24-hour average traffic volume and an 8.2% increase in the peak traffic volume (Fig. 3). On the other hand, it was also confirmed that teleworking reduced commuting by car, in turn reduced gasoline consumption and CO₂ emissions.

[1] Ministry of Internal Affairs and Communications, "Estimates for Internet Traffic in Japan", https://www.soumu.go.jp/joho_tsusin/eidsystem/market01_05_03.html (Day of access: Nov. 26, 2020)

[2] Ministry of Internal Affairs and Communications, "Communications Usage Trend Survey (Companies)", <https://www.soumu.go.jp/johotsusintokei/statistics/statistics05a.html> (Day of access: Jul. 27, 2020)

[3] Persol Research and Consulting Co., Ltd., "Emergency survey regarding the impact of measures against novel coronavirus infection on teleworking", Two times, <https://rc.persol-group.co.jp/news/202004170001.html> (Day of access: Jun. 19, 2020)

[4] NTT East, "Concerning network traffic (back number)" https://www.ntt-east.co.jp/aboutus/traffic/20200414/#area_traffic (Day of access: Jul. 8, 2020)

Factors Affecting CO₂ Emissions from Passenger Cars

Summary

In this proposal, the yearly changes in CO₂ emissions from passenger cars driving were analyzed in terms of three factors: fuel efficiency performance, number of owned vehicles, and travelled distance. As a result, the trend of decrease in CO₂ emissions during 2002 through 2016 could be explained as a whole in terms of a certain amount of effect of the improved fuel efficiency performance on reducing CO₂ emissions, after taking into account the variation in travelled distance, while the effect of increases in the number of owned vehicles has been canceled out. On the other hand, in the analysis of the vehicle lifetime, it was found that the duration for buying a replacement became longer. It can be said that this is rational from the viewpoint of reducing CO₂ emissions because a reduction in CO₂ emissions at the time of vehicle manufacturing can contribute to a reduction of CO₂ emissions throughout the lifecycle. Moreover, in the analysis of a model of user's vehicle selection, it was shown that users' satisfaction of fuel efficiency performance was probably close to saturation.

Proposals for Policy Development

- In addition to conventional measures to promote eco-cars that target the reduction of CO₂ emissions during driving, policies that motivate the reduction of CO₂ emissions during manufacturing are desirable. For users whose annual travelled distance is short, buying a low fuel consumption vehicle for replacement does not necessarily contribute to a reduction in CO₂ emissions throughout the lifecycle, and so there is room for consideration of an amendment to the automobile taxation system, amounting to heavy taxation over the years.
- In order to reduce CO₂ emissions arising from a rebound in travelled distance owing to the spread of low fuel consumption vehicles, it is necessary not only to upgrade vehicles to fuel-efficient ones, but also to introduce a policy applicable for vehicle driving, such as fuel taxation.
- Recently, a trend of decline in users' preference to fuel efficiency performance over the years is recognized. To predict policy effects, it is effective to design policies by taking into consideration changes in users' preferences.

1. Breakdown of factors affecting CO₂ emissions from passenger car driving

The yearly changes in CO₂ emissions from 2002 through 2016 are shown in the amount of itemized contribution of fuel efficiency, traveled distance, and number of owned vehicles (Fig. 1). CO₂ emissions were almost on a declining trend, especially in the 2000s. Improved fuel efficiency contributed to the yearly reduction of the emissions by 0.5 to 1 million tons, but on the other hand, increases in the number of owned vehicles increased emissions.

2. Analysis of service life for vehicles

According to recent data, the service life for vehicles is increasing for the engine displacement range of no more than 2,000 cc, which offsets the CO₂ emission reduction benefits of improved fuel economy from vehicle upgrades. On the other hand, longer service life will contribute to reductions in CO₂ emissions throughout the lifecycle if CO₂ emissions during vehicle manufacturing are reduced. Vehicle updates to a small vehicle with excellent fuel efficiency and its use for a long time is needed. Meanwhile, it was suggested that purchases of low fuel consumption vehicles might result in an increase in traveled distance, giving rise to a rebound in CO₂ emissions.

3. Model of user's vehicle selection

User's vehicle selection was analyzed in the use of a model developed based on utility theory. While the preference for fuel efficiency gradually decreased, users who think positively about fuel efficiency were still predominant.

4. Trend of CO₂ emissions from passenger cars

The CO₂ emissions of the entire vehicle fleet were calculated by adding the CO₂ emissions during driving to the CO₂ emissions at the time of vehicle manufacturing. In addition to the results through 2016, CO₂ emissions from 2017 through 2030 were estimated by way of linear extrapolation (Fig. 2). From the extrapolated CO₂ emissions in 2030, for which the specific reduction of emissions is targeted under the Paris Agreement, it was estimated that the CO₂ emissions from passenger cars may fall by about 38% compared to 2013. The 2030 emissions reduction target for transportation as a whole under the Paris Agreement is 28% compared to 2013; this means that the contribution of passenger cars for the achievement of the target is significant.

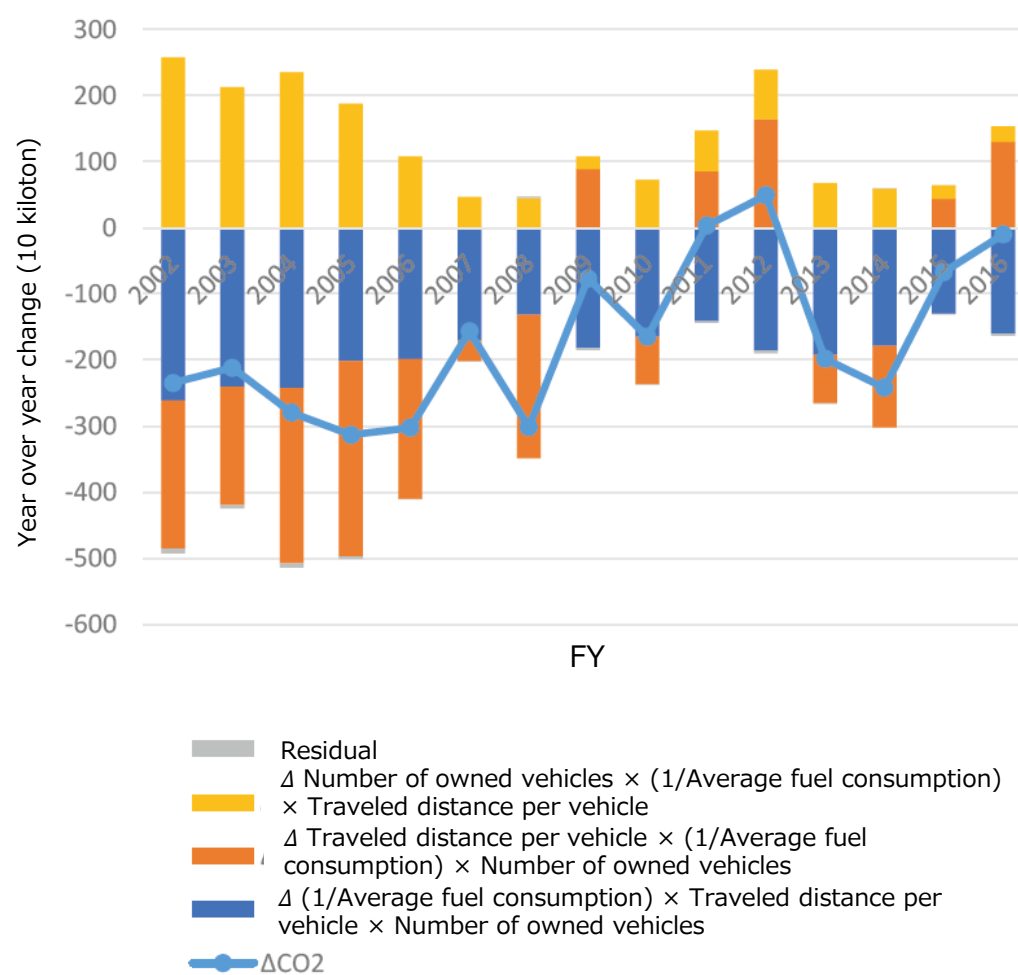


Fig. 1 Breakdown of factors affecting CO₂ emissions from passenger cars

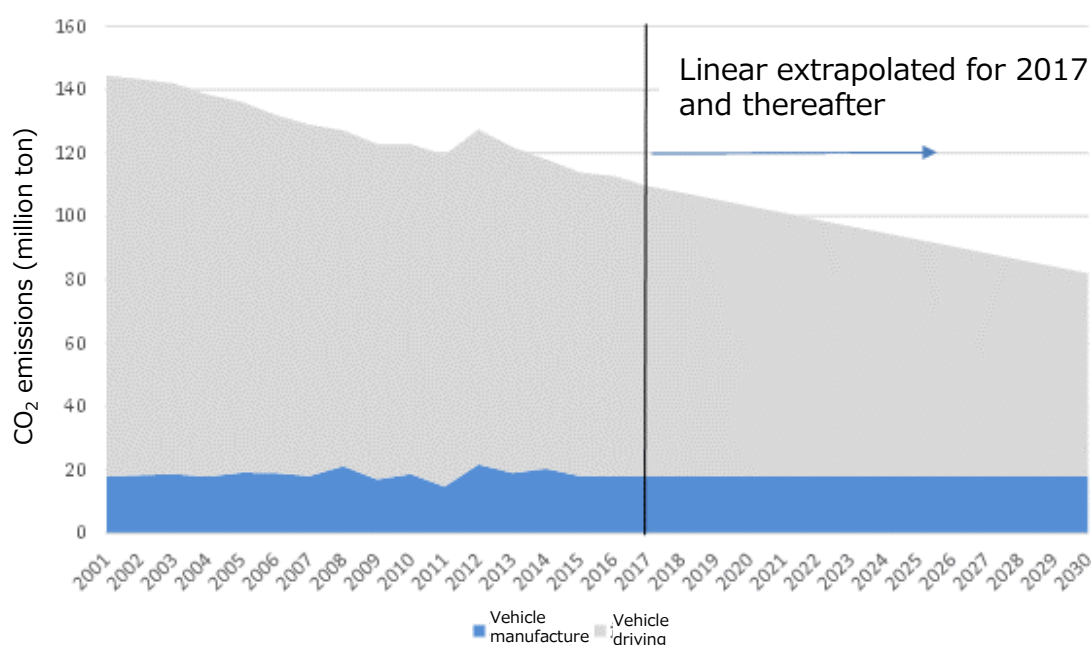


Fig. 2 Changes over the years in CO₂ emissions at the time of vehicle manufacture and during vehicle driving

Survey of Technological Issues in Device Fabrications Processes for Gallium Oxide as a Next-Generation Widegap Semiconductor (Vol. 2): Clarification of Energy Band Diagram of Single-Crystalline Gallium Oxides

Summary

High quality crystals has recently become available for gallium oxide (Ga_2O_3), which is attracting attention as one of the next generation wide gap semiconductor device materials. In this proposal, the energy band diagram of Ga_2O_3 MOS capacitor was clarified by investigating the surface of $\beta\text{-Ga}_2\text{O}_3$ single crystal by means of ultraviolet photoelectron spectroscopy. The interface fixed charge density (N_{int}) of the fabricated capacitors was also estimated experimentally, and it was found that the N_{int} was suppressed to $\sim 1 \times 10^{11} \text{ cm}^{-2}$ with an annealing time of more than 1 hr at 1000°C . It was shown from these findings that the precise understanding of the energy band diagram is important for evaluation of device characteristics.

Proposals for Policy Development

- This time, the energy band diagram of gallium oxide (Ga_2O_3) was investigated, and the device characteristics were evaluated. The obtained interface fixed charge density (N_{int}) and other parameters are not only necessary for improving the device processes, but also indispensable for the exact prediction of device operation and the device design.
- To establish the next-generation widegap semiconductor device technology, it is important not only to accelerate the demonstration of device operation, but also to proceed basic researches for understanding the fundamental properties such as band structure, and the chemical properties such as reactivity, in order to develop a knowledge base available for engineers and researchers working on the properties of those semiconductor materials.

1. Clarification of $\beta\text{-Ga}_2\text{O}_3$ energy band diagram by means of UPS spectrum
 UV photoelectron spectroscopy (UPS) analysis was performed on $\beta\text{-Ga}_2\text{O}_3(001)$ wafers obtained by recent growth technology for large-area wafer (Fig. 1). The low kinetic energy end (cut-off) and the high kinetic-energy end (valence band maximum) of the UPS spectrum were found to be 3.5 eV and 16.5 eV by linear extrapolation respectively, and the valence band maximum energy level, E_V , was estimated is $8.15 \pm 0.02 \text{ eV}$ below the vacuum level. Since the band gap of $\beta\text{-Ga}_2\text{O}_3$ is 4.7 - 4.8 eV [1], it was estimated that the conduction band minimum energy level, E_C , is 3.4 - 3.5 eV deep below the vacuum level.

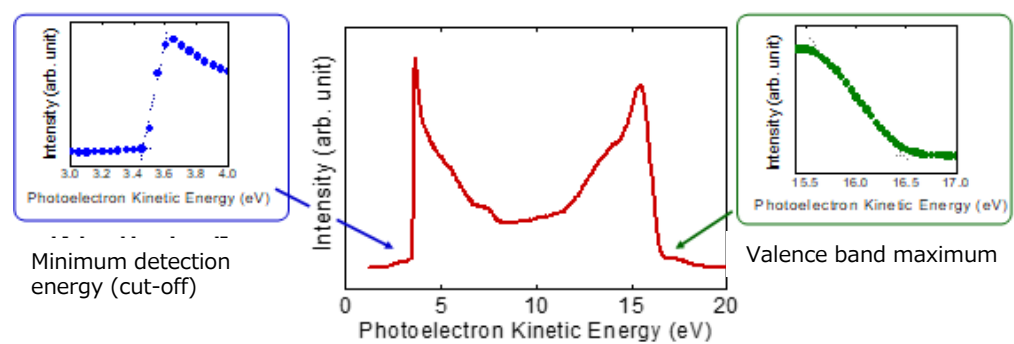


Fig. 1 UPS spectrum on the surface of $\beta\text{-Ga}_2\text{O}_3$ (001) wafer and enlarged views of the spectrum near the minimum detection energy region (left) and near the valence band maximum energy region (right)

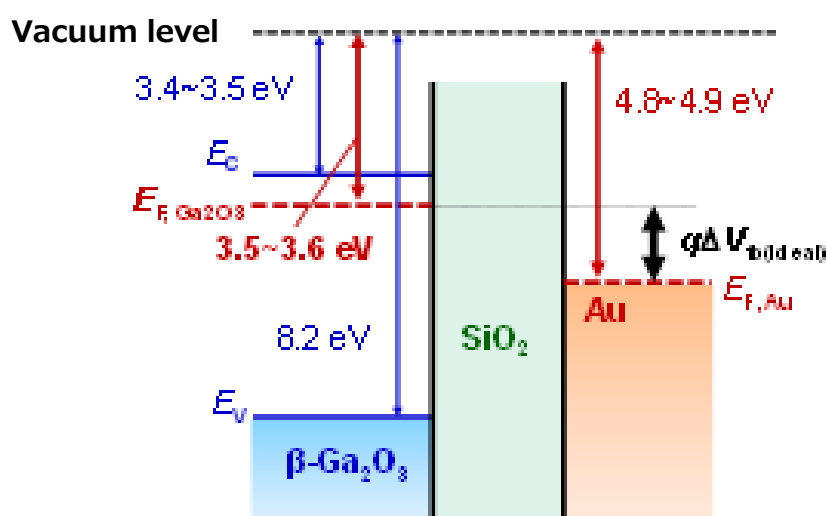


Fig. 2 Energy band diagram of the $\beta\text{-Ga}_2\text{O}_3$ (001) wafer and the fabricated MOS capacitor, referred to the vacuum level.

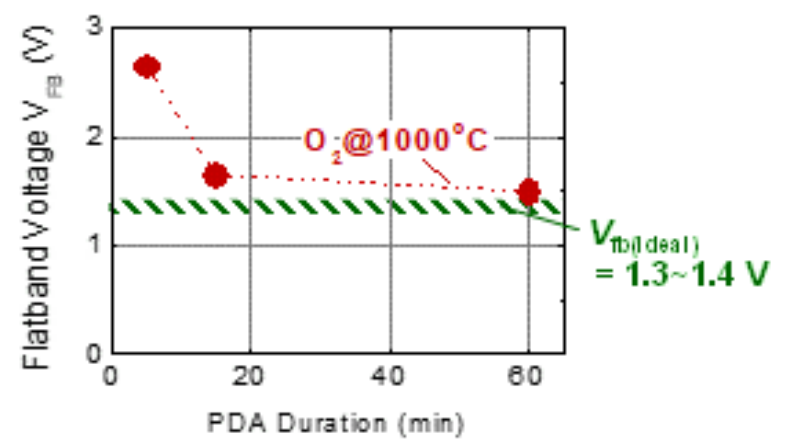


Fig. 3 Relationship between V_{fb} and oxygen annealing duration for Au/SiO₂ (film thickness of about 30 nm)/ $\beta\text{-Ga}_2\text{O}_3$ MOS capacitors

2. Re-verification of device characteristics by estimating Fermi level

Since the difference between the Fermi level $E_{F, \text{Ga}_2\text{O}_3}$ and E_C was calculated to be 0.1 eV, the Fermi level of $\beta\text{-Ga}_2\text{O}_3$ (001) epitaxial film $E_{F, \text{Ga}_2\text{O}_3}$ was estimated to be 3.5 - 3.6 eV deep below the vacuum level. These data are shown in the energy band diagram in Fig. 2.

Finally, the interface fixed charge density (N_{int}) was estimated from CV characteristics of the fabricated MOS capacitors. The fabricated MOS capacitors, Au/SiO₂ (film thickness of about 30 nm)/ $\beta\text{-Ga}_2\text{O}_3$, were used to measure the flat band voltage (V_{fb}) by varying the oxygen annealing duration from 5 minutes to one hour under $1,000^\circ\text{C}$ (Fig. 3). The N_{int} estimated on the basis of the V_{fb} shift from the ideal value ($V_{\text{fb}(\text{ideal})}$) determined using $E_{F, \text{Ga}_2\text{O}_3}$ was minimized to up to $1 \times 10^{11} \text{ cm}^{-2}$ under the condition of annealing duration of one hour. It was clarified from the fabricated MOS capacitor, that the annealing at $1,000^\circ\text{C}$ is effective in reducing the interface fixed charges.

[1] S. J. Pearton, J. Yang, P. H. Cary, F. Ren, J. Kim, M. J. Tadjer, and M. A. Mastro, Appl. Phys. Rev. 5,011301, 2018.

Evaluation on Regional Consumption Structure and Direct and Indirect Carbon Dioxide Emission of Household Sector

Summary

To build a zero carbon emission society, it is necessary to focus on not only direct carbon dioxide (CO₂) emissions by energy consumption in the household sector, but also indirect CO₂ emissions at the stage of manufacturing of consumable goods, such as foods and housing. For the household sector, direct CO₂ emissions were ascertained by region, and indirect CO₂ emissions were ascertained by end-use item, and then a future prediction of them was extended to 2030. Compared to 2015, while direct emissions decreased, the emissions after adding indirect emissions increased. Regionally, the emissions in the urban areas and surroundings increased, but in other regions, particularly in the Tohoku district, emissions were on a declining trend. It is necessary to take global warming countermeasures, getting the whole industry involved, to help to promote reductions of both direct and indirect emissions by taking into account regional characteristics of consumption.

Proposals for Policy Development

- To promote decarbonization while maintaining the economic level, it is desirable to establish a system in which a generous subsidy is allocated to low-income families to make it easy for them to shift to consumption leading to low carbon emissions even if rather expensive.
- The consumption expenditure and CO₂ emissions of the household sector are affected by not only annual income but also regional characteristics, and so it is necessary to establish a system by taking into account regional characteristics, instead of a nationwide uniform system. In addition, the reduction of CO₂ emissions by consumption activities of the household sector may greatly affect not only the electricity generation sector and household sector but also the industrial sector, and therefore it is necessary to promote effective reductions in CO₂ emissions.
- Therefore, for effective policy planning, it is proposed to promote investigation and estimation, in particular by taking into account spatial distribution on the demand side.

1. Estimation of carbon dioxide emissions

Itemized data tabulated in the National Survey of Family Income and Expenditure [1] was used to estimate family expenditure in 2030 by means of multiple regression analysis. Then, based on the estimated family expenditure, CO₂ emissions of the household sector were derived. It was shown that, while direct CO₂ emissions decreased by about 10.2% compared to 2015, the sums of direct and indirect CO₂ emissions increased by 1.3%. Moreover, the sum of direct and indirect CO₂ emissions are summarized for top items in Table 1 [2], and the rate of change relative to 2015 of the sum of direct and indirect CO₂ emissions are plotted by prefecture for four energy-related items in Fig. 1.

When viewing the increase or decrease of CO₂ emissions of the fuel type items, it is shown that the CO₂ emissions per household by "petroleum products" and "city gas" increased in the urban areas and surroundings, but in the Tohoku district, the CO₂ emissions by "petroleum products" and "city gas" decreased, clearly revealing regional variations.

2. Analysis of estimated future scenarios

Three future scenarios were analyzed from the viewpoint of CO₂ emissions from electricity generation or electrification of energy equipment. The total sum of CO₂ emissions of the 47 prefectures was compared among these three scenarios (Table 2).

Table 2 Total sum of CO₂ emissions of the 47 prefectures for three scenarios

	Sum of CO ₂ emissions (million ton CO ₂)	
	Direct emissions	Sum of direct and indirect emissions
Year 2015	208.97	356.39
Year 2030	187.71	361.11
Scenario 1 (70% reduction of CO ₂ emissions from electricity generation)	119.22	230.71
Scenario 2 (Electrification of energy equipment)	161.78	355.57
Scenario 3 (70% reduction of CO ₂ emissions from electricity generation and Electrification of energy equipment)	59.08	187.81

Scenario 1: Based on a prediction that CO₂ emissions associated with electricity consumption can be reduced by 70%, the emission factor of electricity generation CO₂ emissions is reduced by 70%.

Scenario 2: 100% Electrification of "Gasoline" by assuming the shift from gasoline vehicle to electric vehicle (EV), as well as 100% electrification of "City gas" and "Kerosene"

Scenario 3: Scenario 1 + Scenario 2

[1] Ministry of Internal Affairs and Communications, "National Survey of Family Income and Expenditure" <https://www.e-stat.go.jp/stat-search/files?page=1&toukei=00200564> (Day of access: Sept. 12, 2020)

[2] Ministry of Internal Affairs and Communications, "2015 Input-Output Tables for Japan" <https://www.e-stat.go.jp/stat-search/files?page=1&layout=datalist&toukei=00200603&tstat=000001130583&cycle=0&year=20150&month=0> (Day of access: Aug. 24, 2020)

Table 1 Sum of direct and indirect CO₂ emissions for top items

2015 Top Items	CO ₂ emissions (million ton CO ₂)	2030 Top Items	CO ₂ emissions (million ton CO ₂)
Electricity	201.22	Electricity	193.21
Gasoline	73.07	Gasoline	60.00
City gas	37.54	City gas	38.99
Liquefied propane	25.61	Liquefied propane	20.33
Food	11.34	Food	13.56
Kerosene	9.99	Purchase of automobiles	9.65
Water and sewerage charges	7.23	Expenses of repair and maintenance work	9.62
Household head pocket money	6.39	Household head pocket money	7.79
Money gifts	6.10	Money gifts	6.34
Purchase of automobiles	5.71	Water and sewerage charges	6.25

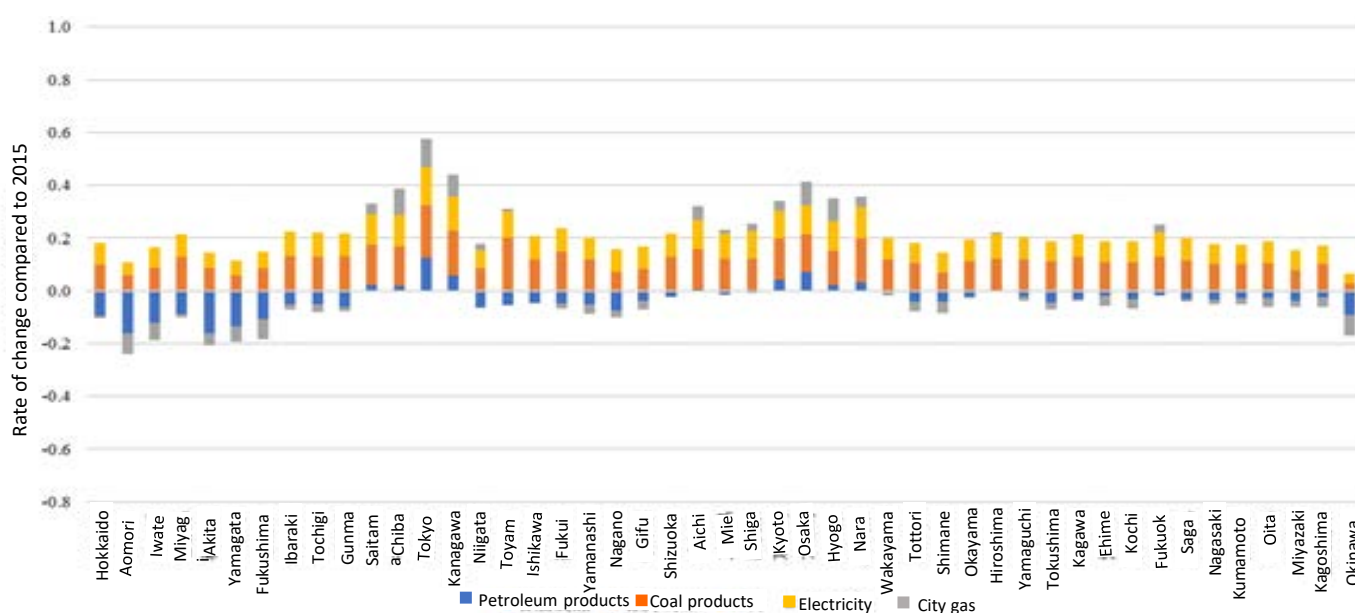


Fig. 1 Rate of change relative to 2015 of the 2030 sum of direct and indirect CO₂ emissions per household

In Scenario 2 of electrification of energy equipment alone, the direct emissions were about 23% reduced compared to 2015, but the sum after adding the indirect emissions remained at about a 0.2% reduction. In Scenario 3, where CO₂ emissions from electricity generation were reduced by 70%, the direct emissions fell by 71.7%, and the sum of direct and indirect emissions fell by 47.3%. At LCS, structural changes throughout the whole industry are examined, including further electrification, such as vehicle electrification, and increase of the proportion of renewable energy in the electricity generation mix. Owing to such structural changes, CO₂ emissions of the household sector will likely change more significantly.

Study on the Effects of Measures to Reduce Timber Production and Distribution Costs Based on a Timber Production and Distribution Flow Model

Summary

In order to establish a sustainable woody biomass system, it is important to expand the use of forest resources within the region, and conceivable measures for this end include ICT-supported operations, mechanization of operations, and smarter distribution. The effects of implementing the measures were analyzed using a flow model developed by means of system dynamics. As a result, the following were found: ICT technology may reduce forest survey costs in the surveys of no less than 40 hectares; introduction of mechanization in production may improve labor productivity by nearly 1.4 times ; introduction of smarter distribution may have an economic effect 0.5 to 1 times greater than the introduction of mechanization. It is probable that these measures may make foresters become economically independent, and eventually encourage the expansion of the use and stable supply of forest biomass resources.

Proposals for Policy Development

- The forest administration in Japan has adopted a system in which the right to own mountain forests is protected, but it is necessary to establish a system, like that in Europe, in which people are accountable for their rights[1]. It is still important to clarify the structure of forest ownership and to take measures to promote the consolidation of operations.
- Consolidation of operations (and the introduction of large machinery to improve production efficiency) and smarter distribution based on matching supply and demand are both equally important as measures to reduce timber production and distribution costs for foresters. In particular, it is necessary to develop and spread a supply-demand matching system which is inexpensive and easy to use even for elderly people, in order to promote smarter distribution.

1. Timber production and distribution flow model

The system dynamics software Vensim was used to graphically represent forestry processes of survey, production (logging), timber distribution, etc. (Fig. 1). The equations and parameters encompassed in this flow diagram can be set according to local conditions, and effects of individual factors on the foresters' annual profits can be analyzed.

2. Creation of individual process models

The following flow model was established to quantitatively evaluate the production, distribution, and other processes discussed in this proposal report among the wood production and distribution processes described in Section 1. (1) Timber production process: Model adopting mechanization needed for production; (2) Timber distribution process: Model adopting "Smarter distribution" to match timber supply and demand, and to allow direct delivery to sawmill by bypassing timber market for part of distribution. Intermediary's expenses, timber market service charges, and other costs can be suppressed.

3. Case study

Using the models created above in paragraph 2, a case study was conducted to verify the effects of individual models by applying the models to the Chusei Forestry Cooperative (an example case of Excellent Tackling Efforts selected by the Forestry Agency), which controls the whole area of Tsu City, Mie Prefecture. Devices for mechanization are given in Table 1 [2], and three scenarios were selected for the "Smarter distribution": current distribution (no direct delivery to sawmill), 60 percent direct delivery, and full direct delivery. Results of the annual income and expenditure simulation per logging volume of 1 m³ are shown in Fig. 2. It was shown that the introduction of mechanization resulted in a nearly 1.4 times improvement of labor productivity (from 5 to 7.06 m³/ man-day), and the introduction of smarter distribution resulted in half to the same comparable effects of cost reduction compared to the introduction of mechanization.

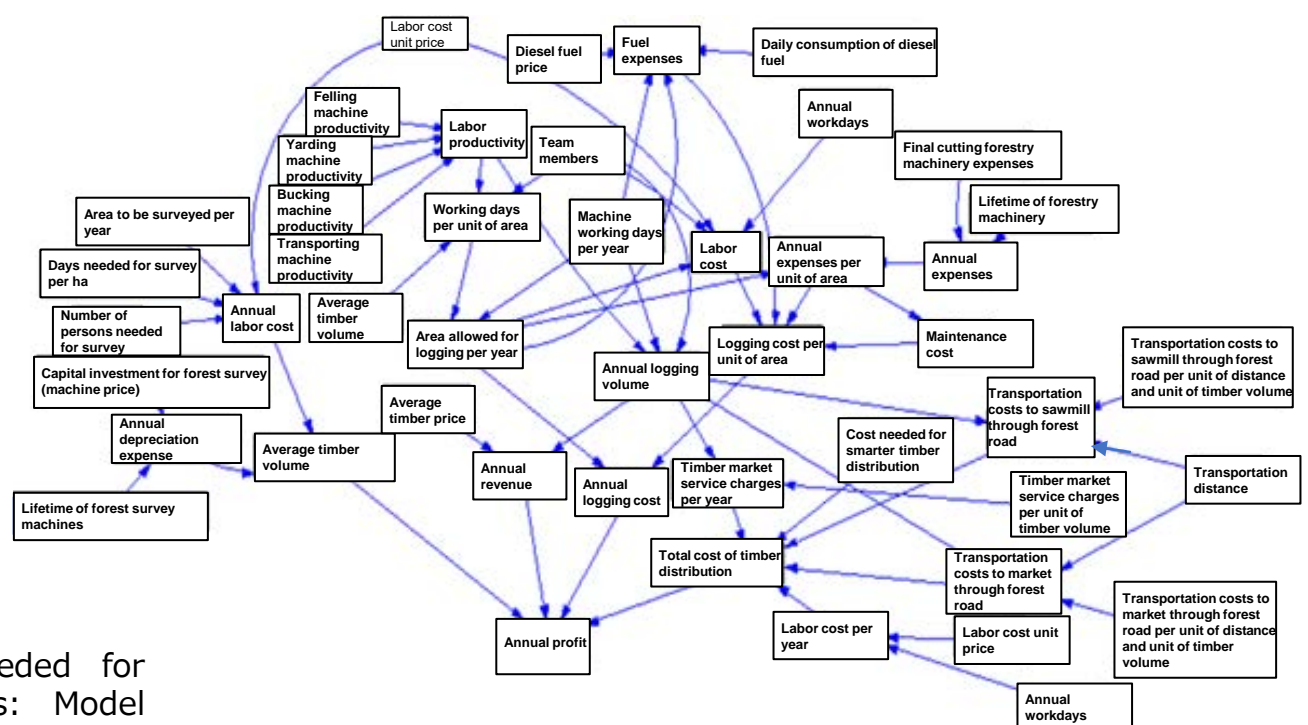


Fig. 1 Overview of timber production and distribution flow model

Table 1 Devices used in the forestry mechanization scenarios

	Felling process	Yarding process	Bucking process	Carrying out process
Before mechanization	Chainsaw	No mechanization		
Mechanization 1	Chainsaw	No mechanization	Forestry processor	Forestry forwarder
Mechanization 2		Grapple skidder		

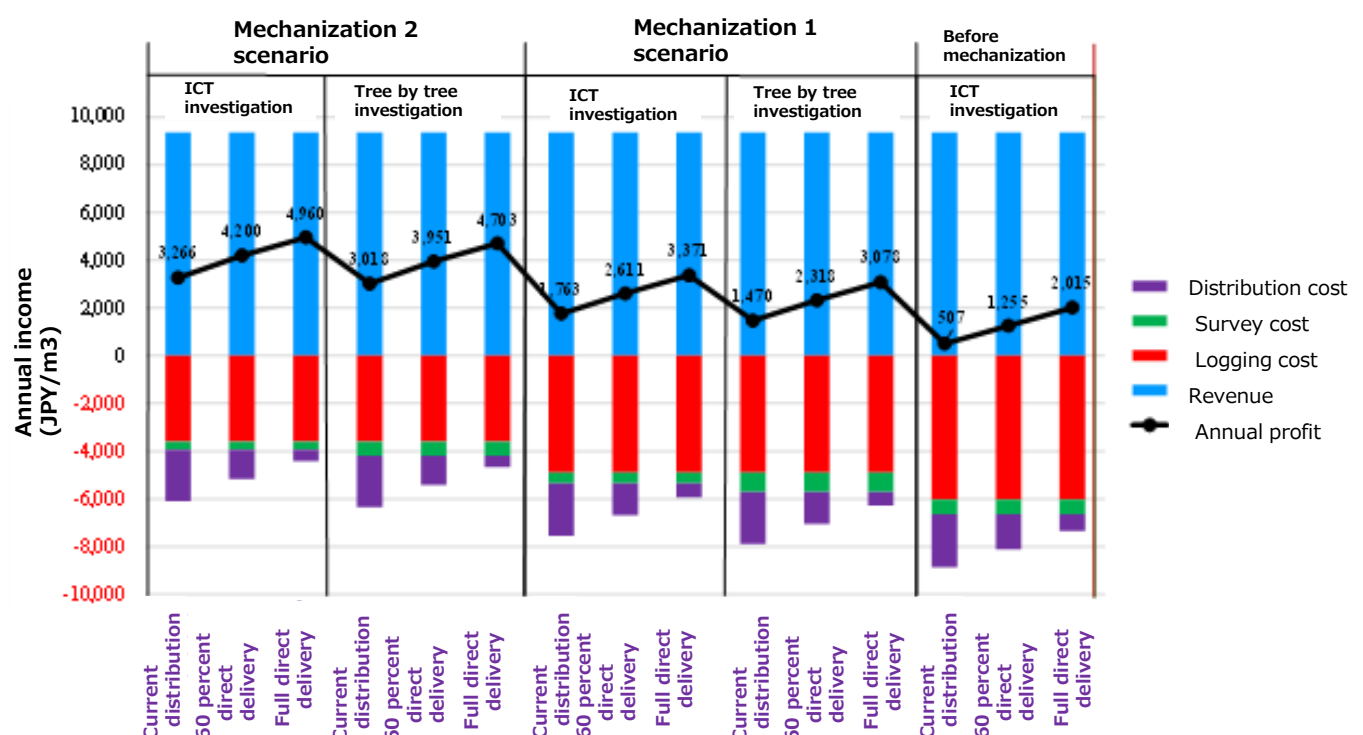


Fig. 2 Results of simulation per logging volume of 1 m³

[1] Hiroshi ISHII, "Development and features of forest policy in France, Germany, and Japan," Forestry Economic Research Vol. 39, No. 1, pp. 3-12, 2003.

[2] Forestry Agency web site, "FY2018 Introduction of Forestry Mechanization Promotion Projects"

<https://www.rinya.maff.go.jp/j/kaihatu/kikai/attach/pdf/30jirei-1.pdf> (Day of access: Mar. 30, 2021)

Proposal of Control Method for Compensating Communication Delay in Load Frequency Control Using Electric Vehicles

Summary

Since the output of renewable power sources fluctuates depending on weather conditions, mass interconnection to the grid raises serious concerns about frequency stability in the grid power. This proposal*) puts forth a control method that directly controls electric vehicles (EVs) using real-time frequency deviation for the EV aggregator (EVA) to compensate for communication delays with the aim of improving the load adjustment capability of EVs, which is considered to be a promising solution in the area of frequency control [1]. As a result of evaluation by dynamic simulation, it was found that the proposed control method can improve the performance score of EVA and reduce the frequency fluctuation at the same time. It was suggested that load frequency control by EVA may be adopted after 2024, when the frequency regulation market is scheduled to be set up in Japan.

Proposals for Policy Development

- Regarding the institutional design of the frequency regulation market, it is necessary to consider the balance for maintaining the stability of frequency control as well as to analyze the advantages and disadvantages of the systems such as PJM and CAISO in the preceding Western countries and to lower the entry barriers for EVA.
- The minimum bid for the Japanese frequency regulation market currently envisioned is 5 MW, which is larger than the 0.1 MW of the US PJM. Until the market matures, reducing the minimum bid to the level of PJM is considered to be an important measure for future EV's participation in the regulation market.

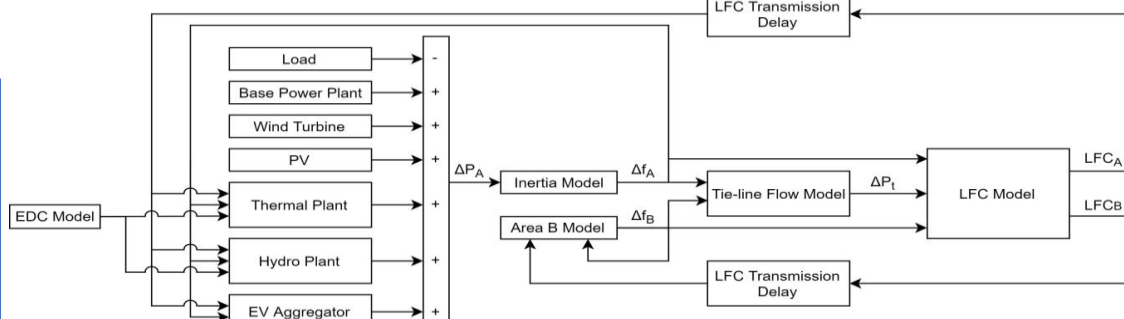


Fig. 1 Grid model diagram

1. Simulation model

The simulation model of the load frequency control system by EVA was examined based on the AGC30 model [2]. As the setting, it was applied that the system load is relatively light and that renewable power sources such as solar power generation and wind power generation are connected to the grid (Fig. 1).

2. Design of load frequency control method by EVA

In the present proposed control method, the parameters are regulated based on the historical data of the received load frequency control (LFC) command and the historical data of the frequency deviation, and the EV frequency is controlled based on the real-time frequency deviation measured from the grid. The logic of the entire control method (Fig. 2) is simple, and it is considered possible to be incorporated into the charge/discharge control system of each EV.

3. Simulation results

The room for improvement in performance of the proposed control method described in Section 2 was examined by simulation in a grid where the flat frequency control (FFC) method is used. In PJM, the performance score is calculated by evaluating the past result of how quickly each frequency regulation resource in the market can follow the LFC command [4], and the present proposal also calculated the performance score by a similar method as the PJM method (Fig. 3). It was found that in each delay time (horizontal axis), the performance was improved as compared with the case where no compensation was performed, regardless of the value of the calculation period t_p .

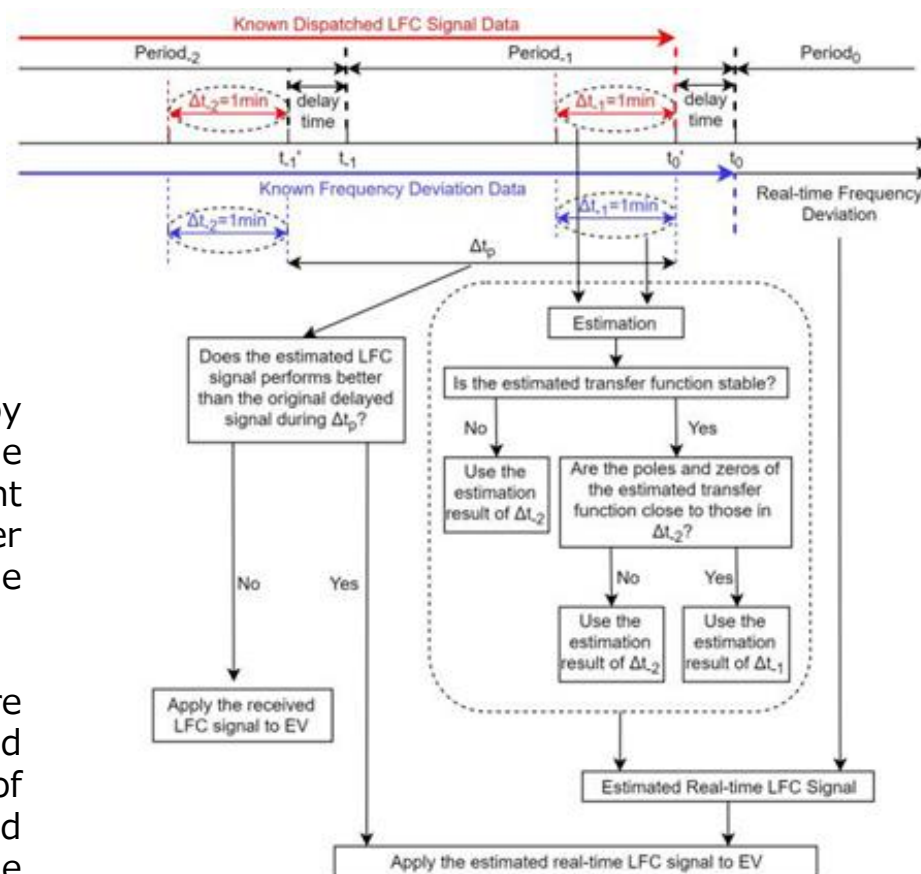


Fig. 2 Control structure in the proposed system

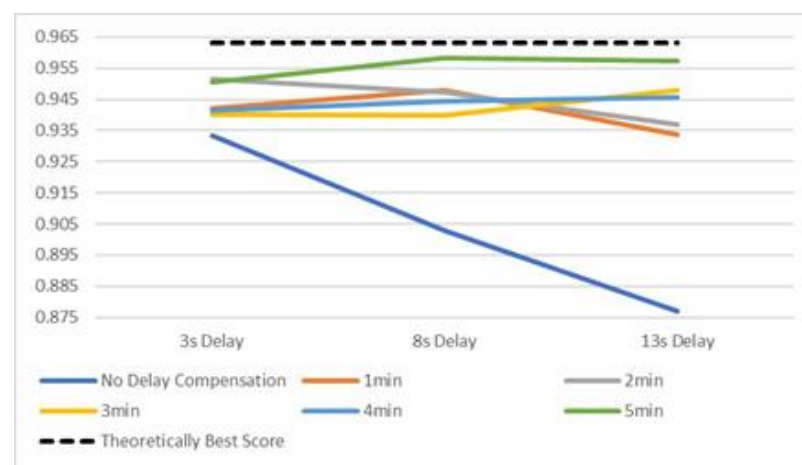


Fig. 3 Performance score (Numbers from 1 minute to 5 minutes are calculation period (t_p))

*) The present proposal is based on the content of the authors' paper in English [1] and is linked to policy implications and policy proposals that will lead to the realization of a low-carbon society.

[1] Sinan Cai and Ryuji Matsuhashi, "A Control Method for Compensating Communication Delays in Load Frequency Control with Electric Vehicle Aggregators", Journal of Society for Energy and Resources, Vol.41, No. 1, pp. 1-10, 2020, https://doi.org/10.24778/jjser.41.1_1.
 [2] Investigating R&D Committee on recommended practice for simulation models for automatic generation control; Institute of Electrical Engineers of Japan Technical Report No. 1386, 2016
 [3] Investigating R&D Committee on load frequency control in a normal time and an emergency in the power grid, "Load frequency control in a normal time and an emergency in the power grid", IEEJ Technical Report, No. 869 (2012), pp.1-147.
 [4] PJM manual 12, "Balancing operations", Revisions:39, 2019.

Economy and CO₂ Emission on Hydrogen Production via Both Coal Gasification and Steam Methane Reforming: Importance of Securing CO₂ Storage Space Domestically

Summary

In hydrogen production processes by coal gasification and steam reforming (SMR) of natural gas, costs and CO₂ load emissions were studied when an amine absorption process was installed, and the CO₂ capture rate was varied in the range of 90 to 99.5%. Additionally, when ZC is achieved with DAC (Direct Air Capture) technologies combined, ZC hydrogen costs and required amounts of CO₂ storage have been calculated separately for an overseas plant location and a domestic plant location. When the overseas storage conditions can be applied to those of the domestic case without any changes, it has been found that ZC hydrogen costs for the domestic case become smaller than those for the overseas case. It is, therefore, important to establish technology and secure locations for domestic storage.

Proposals for Policy Development

■ In order to realize a ZC society, the development of the DAC process is ultimately essential, but at the same time, if the site is domestic, it is necessary to implement CO₂ capture and storage in domestic location, and it is necessary to promote research and development to search for and secure storage sites as well as storage technology.

1. Processes of ZC hydrogen production

Energy consumption, equipment specifications, production costs, CO₂ loads and others were examined for each case of hydrogen production (Table 1). The block diagrams of the hydrogen production process by coal gasification and steam methane reforming (SMR) are shown in Fig. 1 and Fig. 2 [1-3]. Storage areas for captured CO₂ are assumed to be in the vicinity of production plants. In order to achieve ZC, the unabsorbed CO₂ in the amine unit as well as the CO₂ deriving from the production facility must be collected by applying the DAC process.

The hydrogen production was designed for 25.7 t/h (annual production scale of 200,000 tons).

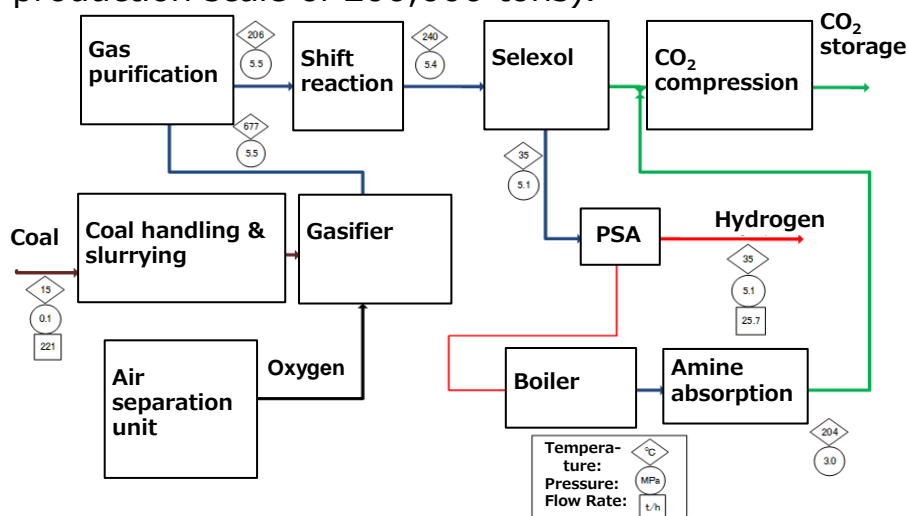


Fig. 1 Block diagram of hydrogen production process via coal gasification

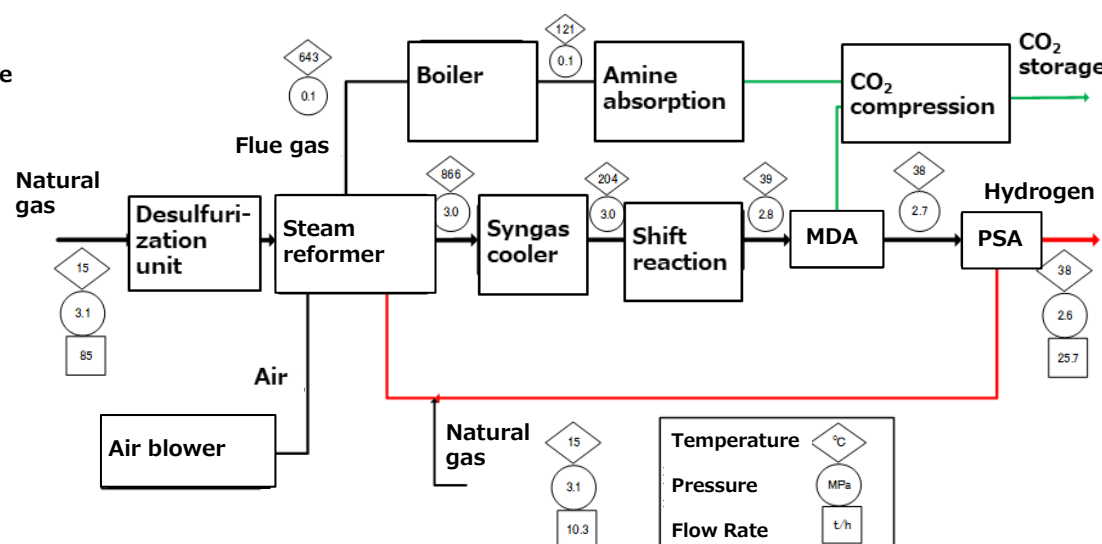


Fig. 2 Block diagram of hydrogen production process via steam methane reforming (SMR)

Table 1 Descriptions of considered cases

	Raw material	Location condition of production plants
Case A	Coal	Overseas
Case B	Natural gas	Overseas
Case C	Coal	Domestic
Case D	Natural gas	Domestic

Table 2 Summary of results

Case	Raw Material	Location	CCS capture efficiency at the production plant (%)	Hydrogen production cost (JPY/MJ)	Transportation cost (JPY/MJ)	DAC cost (JPY/MJ)	ZC hydrogen cost at domestic power station (JPY/MJ)	CCS storage amounts (Mt/y)	DACS storage amounts (kt/y)
A	Coal	Overseas	90~99.5	2.2~2.4	3.7	1.0~0.4	6.9~6.4	3.6~4.0	587~218
B	Natural gas	Overseas		1.2~1.3	3.7	0.7~0.4	5.6~5.3	1.8~2.0	399~214
C	Coal	Domestic		2.1~2.2	—	0.6~0.1	2.7~2.3	Same as A	407~38
D	Natural gas	Domestic		2.8~2.9	—	0.3~0.03	3.1~2.9	Same as B	210~23

2. Hydrogen production costs and CO₂ storage amounts for each case

Results of costs and CO₂ storage amounts for each case are shown in Table 2. The ZC hydrogen costs in domestic power stations of Cases C and D, where production plants and storage areas for captured CO₂ are domestically located with importing coal and natural gas as raw materials, are lower than those of Cases A and B with overseas plants and storage areas. However, the CCS storage amounts to be secured domestically for Cases A and B are equal to the “DACS storage amounts” in Table 2, and those for Cases C and D are equal to the sum of “CCS storage amounts” and “DACS storage amounts.”

[1] LCS, Proposal Paper for Policy Making and Governmental Action toward Low Carbon Societies, “Economy of Hydrogen and Ammonia by Coal Gasification and CO₂ Emissions—A Comparative Consideration on “Economy of Production and Logistics Systems of Hydrogen and Ammonia via Coal Gasification (CCS included)—”, the Japan Science and Technology Agency, the Center for Low Carbon Society Strategy, February 2019.

[2] LCS, Proposal Paper for Policy Making and Governmental Action toward Low Carbon Societies, “Overview and Outlook of CCS (Carbon Capture and Storage)—Assessment and Challenges on CO₂ Separation and Capture Technologies—”, March 2016.

[3] Assessment of Hydrogen Production with CO₂ Capture Volume 1: Baseline State-of-the-Art Plants”, August 30, 2010, DOE/NETL-2010/1434.

Strategy for Hole-Transport-Material-Free Perovskite Solar Cells Using Carbon-Based Electrodes (Vol. 3)

Summary

While perovskite solar cells using carbon-based electrodes have been progressively studied, many challenges remain. In this proposal paper a survey result of some research projects has been completed. One study uses only carbon-based electrodes made of electron conductive materials (carbon nanotubes) with low cost and high stability instead of hole transport material (HTM)/Au electrodes. Another research project provides a functional group-introduced material which improved repeatability and stability of cells. It revealed that the method that adds additives to perovskite films and the method that controls perovskite compositions are both effective. An efficiency of 17% or more has already been reported [1]. Additionally, it has also been shown that the key to high efficiency, high durability and low cost of the perovskite solar cells is to form a strong bonding interface between a perovskite film and an electrode.

Proposals for Policy Development

It is required that research be promoted to solve the following issues regarding the perovskite solar cell using carbon-based electrodes.

- Controlling a defect on a perovskite film
Controlling defects that trap carriers is imperative to obtain more optical current from a photo-excited carrier. Inactivating defects with additives or optimizing perovskite film structures will be more effective measures.
- Optimizing the bonding between perovskite materials and carbon materials
From the perspective of the hole collection rate, materials and structures of HTM-free carbon-based electrodes need to be considered to shut off the electron transfer to carbon-based electrodes instead of the HTM.
- Investigation of high durability mechanisms
HTM/Au electrodes deteriorate due to the diffusion of HTM's dopants or gold atoms, while carbon-based electrodes do so due to carbon exfoliation. It is important that those problematic phenomena be quantitatively studied. It is also necessary to consider cell compositions in line with perpetual changeable features of the perovskite instead of usual stability.

1. Improvement of the perovskite layer

Many studies that use commercially available carbon pastes for solar cells have been reported recently. Some of those report that improved perovskite films or others provide materials with higher efficiencies of 14 to 17% ([2], etc.). Since the perovskite layer has many possible defect structures, passivating a defect with an additive is often used to prevent defect formation. These additives are thought to extend the lifetime of photoexcited carriers as a result of halogen bonding and other interactions that deactivate traps derived from defective structures. Without those additives, inserting a perovskite material $\text{MAPbI}_x\text{Br}_{3-x}$ between MAPbI_3 and carbon also improved the efficiency [1].

2. Junction of perovskite/carbon electrodes

In the case of carbon electrodes, an efficiency of 17.58% was obtained in a study where an inorganic HTM (CuSCN) was tried instead of an unstable organic HTM[4]. The energy levels of perovskite solar cells that use carbon-based electrodes with or without HTM are shown in Fig. 1. Introduction of the HTMs not only blocks the flow of excited electrons to carbon-based electrodes but possibly allows the hole transfer to occur smoothly, because the HOMO level of the HTM is close to that of the perovskite.

3. Structural control of carbon

With carbon modification focused, it has been demonstrated that the usage of carbon nanotube electrodes with oxygen-containing functional groups (-COOH, etc.) can provide strong interaction with PbI_2 thin films. The reconstituted perovskite crystals, in which ions easily diffuse, allow the quality of films and bonding interfaces of solar cells with at most 3% of the initial efficiency to be naturally improved after being left for a long period (Fig. 2), converging to efficiency of 11% or more. Other than the bonding improvement of perovskite layers mentioned above or perovskite/carbon-based electrodes, structure control of carbon-based electrodes is indispensable for enhancing the efficiency and durability.

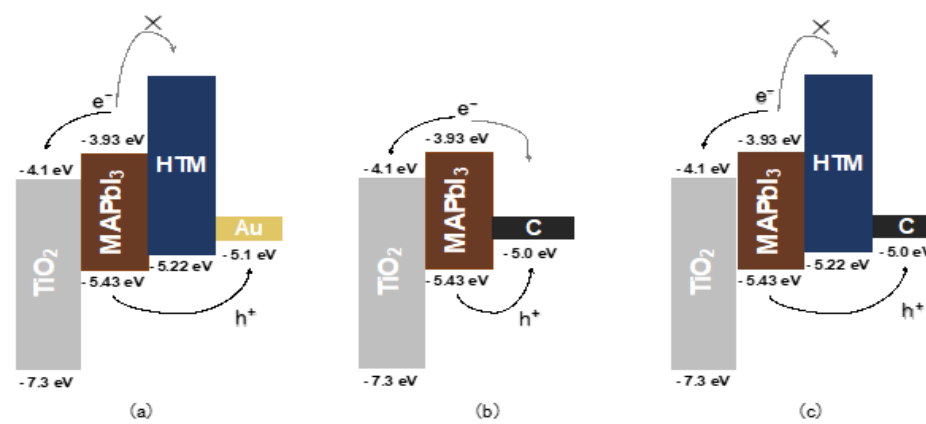


Fig. 1 Energy level of cell constituents

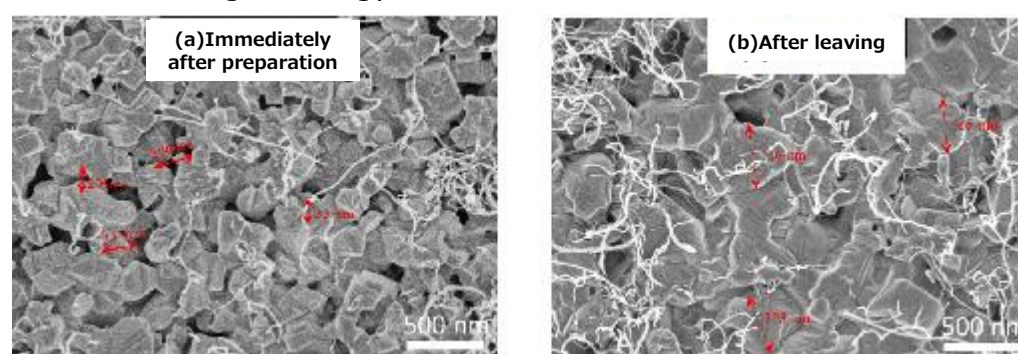


Fig. 2 Electron micrographs of perovskite film surface on the cells using electrodes with oxygen-containing functional groups [3]
(a) Immediately after preparation (b) After leaving

[1] Liu, J. et al. (2019). In situ growth of perovskite stacking layers for high-efficiency carbon-based hole conductor free perovskite solar cells. *Journal of Materials Chemistry A*, 7(22), 13777-13786.
 [2] Liu, C. et al. (2021). Improving the Performance of Perovskite Solar Cells via a Novel Additive of N, 1-Fluoroformamidinium Iodide with Electron withdrawing Fluorine Group. *Advanced Functional Materials*, 2010603.
 [3] Chen, J. et al. (2019). MAPbI_3 Self-Recrystallization Induced Performance Improvement for Oxygen-Containing Functional Groups Decorated Carbon Nanotube-Based Perovskite Solar Cells. *Solar RRL*, 3(12), 1900302.
 [4] Wu, X. et al. (2019), Efficient and stable carbon-based perovskite solar cells enabled by the inorganic interface of CuSCN and carbon nanotubes. *Journal of Materials Chemistry A*, 7(19), 12236-12243.



Economic and Technological Evaluation for Zero Carbon Electric Power System Considering System Stability (Vol. 2):

Scenario Analysis for the Development of Zero Carbon Electric Power System in 2050

Summary

Low carbon and zero carbon electric power (ZC electricity) supply configurations were examined by way of simulating a power supply configuration model, aiming for the economical supply of electricity in 2030 and in 2050. The simulation result showed that it may be possible to supply electricity, at a level below current electricity costs, to meet demand of about 1,700 TWh/y when CO₂ emissions derived from electricity generation fuel in 2030 are reduced by 50% compared to 2013, and of about 1,400 TWh/y when the CO₂ emissions are reduced by 70%. Furthermore, even if for an electricity demand of 1,600 TWh/y in 2050, it may be feasible to construct economical ZC electricity generation configurations. Moreover, an analysis of capital investments showed that, by increasing the reduction of fossil-fuel CO₂ emissions in 2030, the total amount of new capital investments from 2021 through 2029 may be increased by about 20,000 to 40,000 billion JPY.

Proposals for Policy Development

- Towards the achievement of ZC electricity in the future, photovoltaic (PV) and wind power will become the mainstay, and their market sizes will increase. It is important to develop PV and wind power industries strategically considering the expansion of domestic markets in the future.
- While a high demand for storage batteries is expected, the cost of lithium-ion battery is estimated to rise due to depletion of lithium resource. Therefore, an inexpensive and efficient technology that can recycle lithium and promote new power storage technology, and the policy to realize large-scale power storage systems are required.

1. Power supply configuration and power cost calculation

Linear programming method was used to determine a power supply configuration that minimizes the generation cost by using input data of electricity demand per hour in a typical day for every season at every region in Japan. Table 1 shows the parameters for the power supply configuration model. Table 2 shows the power supply configuration breakdowns and costs for typical cases of power demand. For the 2030 cases of A, C, and D, the electricity cost was lower than the electricity cost in 2018 (13.9 JPY/kWh [1]). For the 2050 case of E, the electricity cost was 15 JPY/kWh including the transmission cost for the electricity demand of 1,000 TWh/y, about the same as in 2018.

Table 3 Six scenarios of electricity generation configuration until 2050

Scenario	Case		Electricity demand [TWh/y]		Reduction of fossil-fuel CO ₂ emissions [%-2013]	
	2030	2050	2030	2050	2030	2050
1	A	E	1,000	1,000	36	100
2	C				50	
3	D				70	
4	A				36	
5	C				50	
6	D				70	

Table 4 Amounts of new capital investments from 2021 through 2049 [1,000 billion JPY]

Scenario	1	2	3	4	5	6
2021 - 2029	LNG	12	14	9	15	12
	PV	20	14	28	26	41
	Wind Power	2	0	12	3	3
	Storage Battery	6	3	11	7	7
	Others	0	0	0	0	0
	Subtotal	41	31	60	51	53
2030 - 2049	LNG	0	0	0	0	0
	PV	24	24	24	56	56
	Wind Power	40	40	40	64	64
	Storage Battery	10	9	11	22	25
	Others	31	31	31	53	53
	Subtotal	104	104	105	194	194
Total	145	135	166	245	247	

Table 1 Parameters used for the electricity generation configuration model in this proposal

Case	A	B	C	D	E
Year	2030				2050
Cost level [year]	2025				2030
Reduction of fossil-fuel CO ₂ emissions [%] compared to 2013	36		50	70	100
Lower limit of inertial force ratio [%]	25	50	25		25
Upper limit of electricity demand [TWh/y]*	2,125	2,055	1,705	1,385	2,770
LNG electricity generation	Yes				No
Nuclear power generation	Yes**		No		No
Coal fired power generation	Yes		No		No
PV potential [GW]	693				1,386
Onshore wind power generation potential [GW]	262				262
Fixed-bottom offshore wind power generation potential [GW]	0				95
Floating offshore wind power generation potential [GW]	0				538
Biomass power generation endowment [TWh/y]	34				40
New pumped storage power generation potential [GW]	0				282
Hot dry rock geothermal power generation potential [GW]	0				21.7
NH ₃ turbine	No				Yes
Reinforcement of inter-region transmission network	No				Yes

*Upper limit of electricity demand that can be achieved with CO₂ reduction and inertia constraints in each case (confirmed in increments of 5 TWh/h)
 **Some were calculated with "No".

Table 2 Electricity generation capacity and electricity cost for typical electricity generation configurations

Case	A						C			D			E		
Year	2018						2030						2050		
Rate of reduction of CO ₂ emissions from power generation fuel compared to 2013	36%						50%			70%			100%		
Electricity demand [TWh/y]	1,107	1,000	1,200	1,600	1,900	1,900	1,000	1,200	1,600	1,000	1,200	1,385	1,000	1,600	2,000
Electricity generation capacity [TWh/y]	Nuclear Power	62	0	0	0	149	-	-	-	-	-	-	-	-	-
	Coal	924	237	138	0	0	0	-	-	-	-	-	-	-	-
	Existing LNG	110	277	376	355	356	285	292	251	238	230	199	-	-	-
	Newly-established LNG	-	273	337	559	580	580	443	440	480	204	210	240	-	-
	Hydropower	78	92	92	92	92	92	92	92	92	92	92	92	92	92
	PV Power	65	299	373	536	636	656	214	393	648	401	579	671	491	1,142
	Wind power (onshore)	11	29	35	119	186	296	0	36	221	119	165	284	443	558
	Wind power (offshore)	-	-	-	-	-	-	-	-	-	-	-	-	66	214
	Geothermal power	2	11	11	11	11	11	11	11	11	11	11	11	11	11
	Woody biomass power	20	0	0	0	0	21	0	0	0	0	0	28	53	35
Total	1,162	1,050	1,262	1,693	2,008	2,010	1,044	1,263	1,702	1,064	1,287	1,525	1,256	2,166	
Usage [TWh/y]	Storage battery	-	72	90	132	177	209	10	83	240	140	249	297	176	385
	Pumping-up power	10	0	0	0	0	2	0	0	1	0	1	8	93	247
	NH ₃ Turbine	-	-	-	-	-	-	-	-	-	-	-	-	11	32
Storage battery facility capacity [GWh]	-	265	316	463	618	822	141	313	865	500	889	1,145	521	1,211	
Electric generation cost [JPY/kWh]	13.9	10.0	10.3	10.9	11.4	11.6	10.7	10.7	11.6	11.4	12.0	13.0	13.0	15.0	
Electricity transmission cost [JPY/kWh]	1.0	0.6	0.7	0.6	0.6	0.7	0.5	0.6	0.7	0.7	0.8	0.8	1.6	2.0	

*Including petroleum, etc.
 ** Calculated assuming no nuclear power operation

2. Changes in capital investments and CO₂ emissions

Based on the electricity power supply configuration given in Table 2, the amounts of new capital investments and CO₂ emissions until 2050 were calculated for each scenario assuming a combination of electricity demand and fuel CO₂ emission reduction rate (Table 3). Comparing the total amounts of capital investments until 2049 (Table 4), the total amounts of capital investments for scenarios 3 and 6 in which the fossil-fuel CO₂ emissions are reduced by 70% in 2030, were about 1.1 to 1.2 times those for the scenarios of 1 and 4, in which the fossil-fuel CO₂ emissions are reduced by 36%, respectively. This means that related markets may be highly activated by increasing the reduction of CO₂ emissions. Although the fossil-fuel CO₂ emissions are assumed to be zero in 2050 in these scenarios, CO₂ emissions associated with facility construction remain, suggesting that it becomes more important to develop technologies to suppress facility construction CO₂ emissions in the industrial fields towards the realization of ZC electricity.

[1] LCS, Proposal Paper for Policy Making and Governmental Action toward Low Carbon Societies, "Economic and Technological Evaluation for Zero Carbon Electric Power System Considering System Stability (Vol. 1)," Center for Low Carbon Society Strategy, Japan Science and Technology Agency, March 2020.

Direct Synthesis of Organic Substances by Hydrothermal Treatment of CO₂-Rich Absorbent from CO₂ Capture Process

Summary

In order to establish an energy-saving and low-cost carbon dioxide capture and utilization (CCU) technology for CO₂ emission reduction, direct synthesis of organic substances by way of hydrothermal treatment was proposed, and the effectiveness was experimentally verified. In this process, the reaction called direct hydrothermal treatment between carbon dioxide and water which is accelerated in the presence of a reductant and a catalyst under high temperature and high pressure, is combined with CO₂ absorption by means of an alkali carbonate absorbent, to simultaneously synthesize organic compounds such as formic acid and to regenerate the absorbent. In preliminary experiments of synthesis by hydrothermal treatment of potassium bicarbonate (KHCO₃) solution along with a reductant and a catalyst, a formic acid yield of 32.7% and an absorbent regeneration rate of 77.8% were obtained, although 100% recycling of alkali carbonate absorbent was difficult to attain.

Proposals for Policy Development

For further examination in the future, the following research should be advanced:

- Because the absorbent solution is not 100% recyclable, a synthetic process in combination with CO₂ absorption should be designed.
- Recovery of the produced formic acid and regeneration of the oxidized reductant will also be investigated. In addition, the energy input and CO₂ emissions are evaluated to assess the feasibility of the CCU process.
- Fe powder was used as the reductant in this process, but the cost should be compared with that when hydrogen derived from renewable energy is used as a reductant. Moreover, added value by generating formic acid and hydrogen, instead of consuming Fe will be considered, and also from an economic point of view, the advantages of the proposed process over other CCU processes will be discussed and proposed.

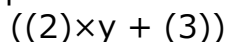
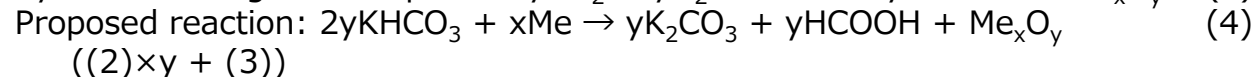
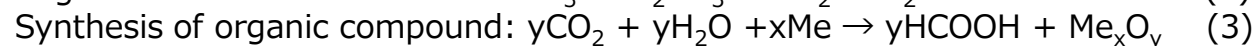
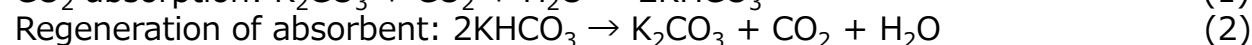
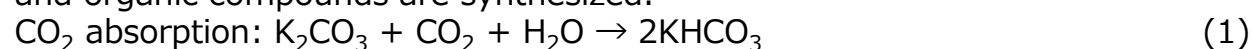
1. The proposed process

Figure 1 shows a general CCU process. Problems to be tackled include consumption of energy when the absorbent is regenerated, and the large transportation energy and cost to the CO₂ separation and recovery site and to the site where CO₂ is converted to organic matter. The organic compound synthesis technology process by way of hydrothermal treatment (Fig. 2) remains advantageous in terms of energy and cost needed for the process and transport of CO₂.

2. Discussion on the hydrothermal treatment of CO₂ chemical absorbent

Equation (1) shows the reaction of CO₂ when K₂CO₃ solution is used as the chemical absorbent. By heating to high temperature or reducing the pressure to release CO₂, highly pure CO₂ is captured, and the absorbent is regenerated

(Equation (2)). Furthermore, by reducing CO₂ with a metal, organic compounds such as formic acid can be synthesized (Equation (3)). In this study, a process (Equation (4)) was proposed, in which reactions (2) and (3) are carried out as a one-stage process, whereby K₂CO₃ is regenerated from the absorbent by hydrothermal treatment of KHCO₃ solution, generated in the reaction (1), under high temperature of more than 250°C and high pressure, and organic compounds are synthesized.



3. Experiment details, results and discussion

In the experiment, KHCO₃ was used as the CO₂ source, Fe powder as the reductant, and Ni powder as the catalyst. The CO₂ source concentration was varied from 0.5 to 2.0 M, the range used in the chemical absorption process, and the reaction tube was inserted into the electric tube furnace, and the reaction was continued for 120 minutes under the temperature of 300°C. The experiment was conducted twice for each reaction condition, and the average values of the formic acid yield and the rate of regeneration of absorbent were calculated (Figs. 3 and 4).

It is recognized in Fig. 3 that the formic acid yield showed a trend of increase as the KHCO₃ concentration was increased, and the value of 32.7% was attained for the concentration of 1.0 M. Concerning the rate of regeneration of absorbent shown in Fig. 4, the rate of regeneration of absorbent increased as the KHCO₃ concentration was increased from 0.5 to 1.0 M, the maximal value of 78% was attained for the concentration of 1.0 M, and the rate of regeneration decreased as the KHCO₃ concentration was increased from 1.0 to 2.0 M. This finding suggests that, in the region up to 1.0 M, the consumption of CO₂ is faster than the consumption of the raw material of bicarbonate ion, thereby reaction (2) is accelerated giving rise to an increase of rate of regeneration. In the region over 1.0 M on the other hand, the consumption of HCO₃⁻ is faster than the consumption of CO₂, thereby the quantity of carbonate ion is reduced in the equilibrium of reaction (2) giving rise to a decrease of rate of regeneration.

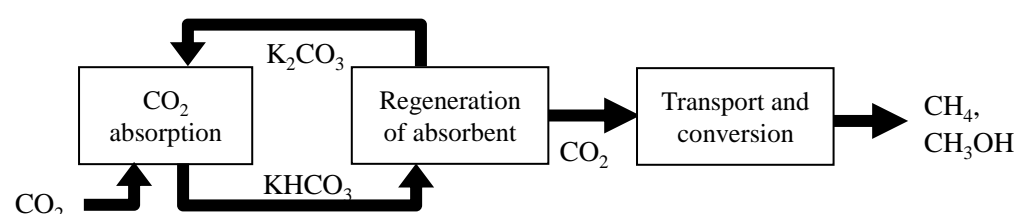


Fig. 1 Conventional CCU process using chemical absorbent

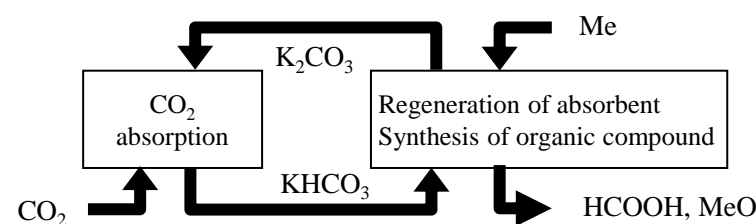


Fig. 2 CCU process using chemical absorbent, proposed in this study (Me: metal)

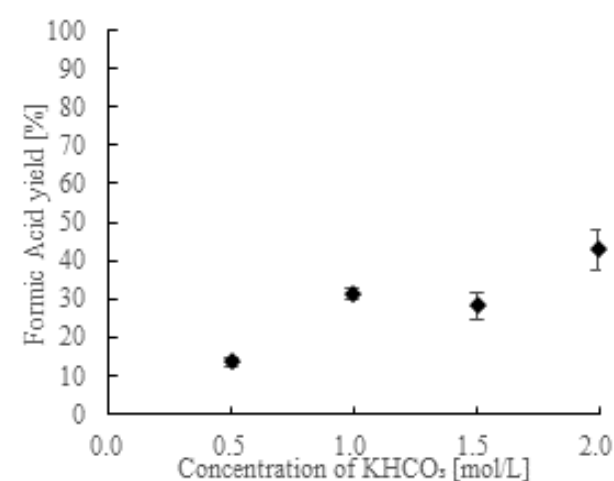


Fig. 3 Relationship between KHCO₃ concentration and formic acid yield (Error bar indicates standard deviation)

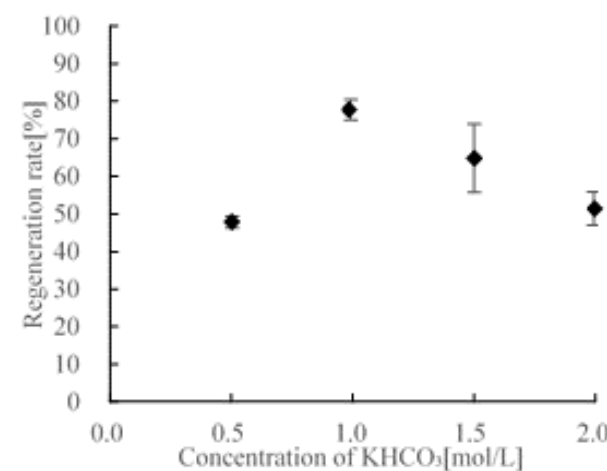


Fig. 4 Relationship between KHCO₃ concentration and rate of regeneration of absorbent (Error bar indicates standard deviation)

• The present proposal is compiled for policy making, using the data of the authors' conference presentation [1].

[1] Akutsu, Shimada, Nagata, Fukunaga, and Takahashi, Effects of concentration of alkali carbonate absorbent in hydrothermal synthesis of formic acid from CO₂, 52nd Autumn Meeting (Okayama), Society for Chemical Engineers, Japan, 2021.

An Expansion of Input-Output Model Focusing on the Demand-side Structural Changes (Vol. 1): Changes of Input-Output Coefficients and Capital Formation Coefficients and Model Development

Summary

It is widely recognized that effecting a shift from a “low-carbon society” to a “zero-emission society” requires not only replacing the existing equipment with more energy-saving and emission-reduction equipment, but societal changes, which involve the participation of consumers enhancing the use of information and communication technologies (ICTs). A wider application of ICTs in industrial and household sectors, the deployment of electric vehicles (EVs) and other new types of automobiles as well as the development of associated infrastructure, are examples that are expected to contribute to low carbonization. In this proposal, we constructed an extended input-output analysis model imposing information technology and energy demand changes in the household sector. Capital formation structure changes are also included. We then calculated the preliminary overall assessment of the industry in 2030. Whereas the results show the zero-emission scenarios for individual industries, it was suggested the necessity of in-depth investigation of zero-emission in the process systems of petroleum products, chemical industry, and others, and then incorporation into the context of the input-output table for the establishing of a socio-economic scenario.

Proposals for Policy Development

- The necessity of various options of new technologies spread in society is recognized, but two further problems are raised.
- The first is the change in the stock of existing equipment and the speed of introducing new equipment. When the introduction of new equipment is hastened, incentives for this need to be provided in the system.
- The second involves spillover effects due to the introduction of new products. This time, the input of petroleum products as raw material was on an increasing trend. Although the introduction of petroleum products does not directly contribute to CO₂ emissions, some sort of measures will be needed before the stage of final disposal.

1. Incorporation of new technology options into the input-output analysis

The information necessary for the evaluation of incorporation of each technological issue given in Table 1 was assigned to the process, which is currently underway at LCS, creating a quantitative socio-economic scenario for achieving a zero-emission society. Focusing on an intermediary stage in 2030, data required were estimated, and incorporated into the input-output analysis model.

2. Construction and estimation of input-output Models

An input-output analysis model was created for quantitative evaluation of a total industrial picture,

which was composed from the information of input-output coefficients, capital stock prediction, capital coefficients, final consumption of each technological elements. According to the simulation results for the growth of Scn-1 through Scn-5 shown in the Fig. 1, scenarios of Scn-1 and Scn-2, in which productivity improvement is absent until 2030 and industrial growth is made only through capital accumulation, stayed in an annual rate of from 0.4% to 0.5%. For the scenarios of Scn-3, Scn-4, and Scn-5, which include labor productivity improvement due to ICTs such as SaaS, based on a survey conducted by the Ministry of Internal Affairs and Communications, the increase of about 28% over 15 years was observed. In addition to the rise in the output value of the passenger car sector due to the introduction of new automobiles with high unit prices, general-purpose machinery, production machinery, and industrial electric equipment, in which Japan has a competitive edge, are growing. In terms of electricity consumption, there was an overall increase due to electrification, but there was significant growth in the chemical industry and rather a decline in the electronics industry. In the above preliminary study, it can be said that the characteristics of the input-output analysis were utilized as the zero-emission scenario for each industry was presented, although there are still issues to be addressed in the process industries.

Table 1 Information used for linking technological options to the input-output analysis model

	Input-output coefficient	Capital formation coefficient	Final consumption	Stock for future	Others
① Information service for consumer			○		
② Information service for enterprise					(*)
③ Transport service (MaaS)	○	○	○		
④ New types of automobiles like EV and PHEV	○	○	●	○	
⑤ Zero energy housing (ZEH)	△	○	●	○	
⑥ Trucks	○	○	●	○	
⑦ Final consumption of fossil fuel in the industrial sector	○				

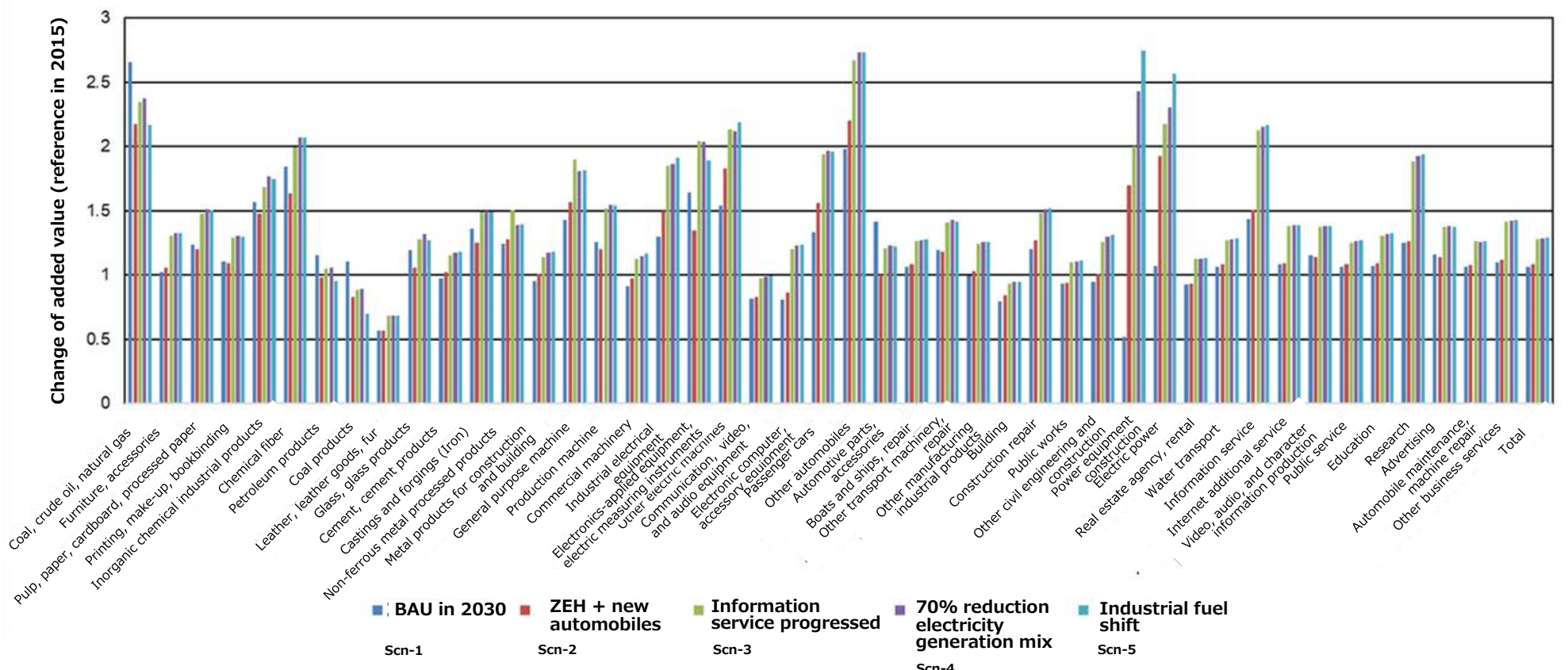


Fig. 1 Ratio of relative change in production of added value from the reference in 2015 by sector for five scenarios

Estimation of the Installation Potential of Solar Cells Reflecting Shadow Effect, Geographic Information, and Latest/Future Technology Trends: Analysis in Tokyo Area

Summary

In order to maximize the introduction of photovoltaics (PVs) power in urban areas with high electricity demand and a large grid capacity such as Tokyo, it is important to estimate the potential to install PVs in the buildings. As a result of quantifying the effect of shadows between buildings in order to consider the installation to the wall surface and estimating by assuming the average efficiency of solar cells by 2030 as 25.5% and the installation cost as 128,000 yen/kW, the potential of installing PVs in Tokyo was 91.1 GW and the annual power generation was 79.5 TWh. This amount of power generation almost covers the power demand (83.6 TWh) [1] of Tokyo in 2019. In addition, as a result of estimating the changes in the potential of installing PVs and the cumulative installation amount corresponding to the improvement of the PV power generation efficiency and the change in the installation expansion rate, it was estimated that the potential of installing PVs will decrease if the installation expansion precedes and the power generation efficiency improvement is delayed. It was suggested that it is important to develop technology to improve the maximum power generation efficiency in addition to the installation expansion.

Proposals for Policy Development

- Assuming that the efficiency of solar cells newly installed in 2030 will be improved by about 25%, it was found that there is a potential to secure 100% or more of the power demand by combining wall installations in residential areas in Tokyo. Therefore, it is appropriate to set challenging goals for the installation of PVs toward 2030 and 2050.
- Since securing a balance between supply and demand of renewables between the seasons is also an urgent issue, it will be necessary to promote the installation expansion of PVs on the building-wall surface.
- In PV, it was found that the improvement rate of the conversion efficiency and installation speed of solar cells affect the final installation potential, so it is required to promptly proceed with research and development to improve the conversion efficiency of solar cells while maintaining costs.

1. Calculation of PV power generation installation potential considering the effects of shadows

In estimating the installation potential (Fig. 1), each city, ward, and village in Tokyo was included in the calculation range, and the wall surface (height above 3 m above the ground) and roof (directly above the roof) were included in the calculation. The amount of solar radiation every 15 minutes was calculated every 15 days for a year, and the total solar radiation on the installation surface and the total power generation when the power generation efficiency was set to 25.5% were estimated (Table 1). The total solar radiation on an installable wall surface was 0.35 times that of a rooftop for residential systems, 0.53 times for public facility systems (high-rise buildings, etc.), and 0.27 times for public facility systems (schools, factories, etc.). The annual power generation in Tokyo was 79.5 TWh, compared to the Ministry of the Environment's estimation of 11.7 TWh [2].

2. Change of installation potential due to improvement of power generation efficiency and installation expansion scenario

Multiple scenarios for technological development (improvement of power generation) and scenarios for installation expansion were created, and how the installation potential changes under each scenario was examined (Fig. 2).

In cases where the installation expansion is accelerated, if technological innovation is slow, the proportion of panels installed with low efficiency will increase, and the installation potential will eventually decrease. In cases where the installation expansion is slow, the influence of slow technology innovation will be reduced, but the installation will be significantly delayed as a whole. Furthermore, it was found that when technological innovation becomes sluggish, the average efficiency further decreases.

[1] Agency for Natural Resources and Energy, Electricity Survey Statistics Table (2019), https://www.enecho.meti.go.jp/statistics/electric_power/ep002/results.html

[2] Entrusted Work Concerning the Development and Disclosure of Basic Zoning Information Concerning Renewable Energies, Ministry of the Environment (2019, etc.) <https://www.jst.go.jp/lcs/pdf/fy2020-pp-20.pdf>

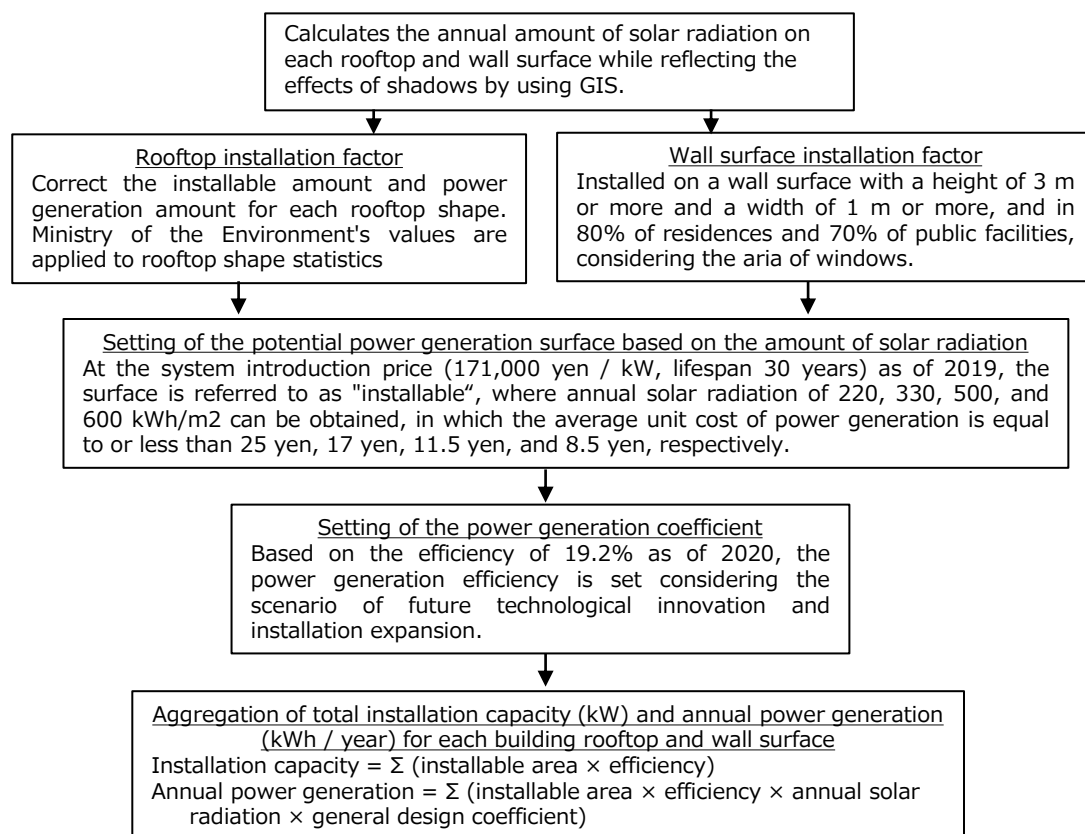


Fig. 1 Outline of installation potential estimation

Table 1 Installable area, total solar radiation and installation potential, and annual power generation in Tokyo (efficiency is set as 25.5% (existing facility: 16.6%))

		Total area [km ²]	Installable area [km ²]	Installation area total solar radiation [TWh/year]	Installation potential [GW]	Annual power generation [TWh/year]
Ministry of the Environment	Residential rooftop	173.0	98.5	118.4	8.3	9.6
	Residential wall surface	-	-	-	-	-
	Public facility rooftop	46.6	36.0	32.2	2.6	2.36
	Public facility wall surface	-	6.7	7.4	0.49	0.54
This survey	Residential rooftop *	176.4+32.0	158.0	180.2	34.5	40.9
	Residential wall surface	257.7	122.7	66.1	27.5	14.8
	Public facility rooftop**	24.4+58.5	20.0+46.9	22.7+54.6	4.2+10.1	4.9+11.7
	Public facility wall surface	3.3 + 12	3.3 + 12.0	6.2 + 29.1	2.5+12.2	1.4+6.5

*Ministry of the Environment excludes houses with a rooftop area of less than 50 m²

**Public facilities (schools, factories, etc.) and Large-scale buildings

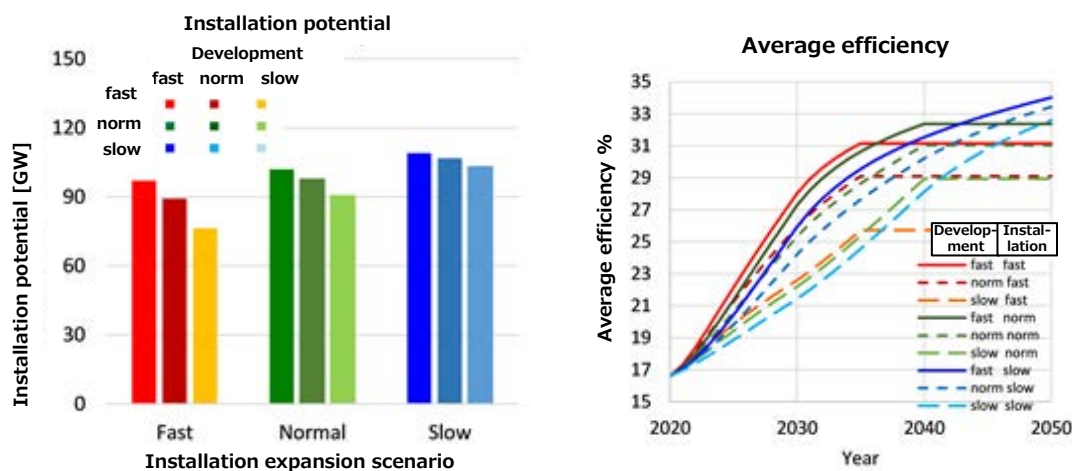


Fig. 2 (Left) Power generation efficiency improvement scenario, installation potential for each installation speed scenario; (Right) Average efficiency of installed solar cells for each scenario